Response to Referee Comments for
"Design and analysis of a spatially heterogeneous wake"

Corresponding author: Alayna Farrell

November 5, 2020

Abstract

The authors would like to thank the referees for their comments. The authors believe that this paper is much improved by addressing the referees' concerns.

1 Referee 1:

General comments:

This paper presents an interesting improvement of the FLORIS wind farm model with the implementation of a method to take into account an heterogeneous atmospheric inflow. The original wind farm model is well described and efforts have been made on the description of the new implementation with plots that are quite useful for the comprehension, but there are still grey areas and it lacks information about the processing of the z-dimension for the complex terrain application: this application is mentioned twice in the introduction and in the conclusion, and the test case is a wind farm in complex terrain, but no information is given on this specific point. While the test case lacks some detailed information about the wind farm and the atmospheric conditions, a comprehensive comparison has been performed between the original homogeneous FLORIS and the two presented improvements. An exhaustive presentation of quantitative indicators is given and the authors provide well-detailed explanations and conclusions.

Thus, more explanations should be given on the wind direction change processing and the processing of the vertical dimension should also be addressed if a potential application remains "wind farms in complex terrains". Therefore I suggest a major revision.

Here are some general suggestions:

- In the introduction, the authors could mention other state-of-the-art wake modeling utilities and give more general information on the heterogeneity part with reference to studies on the characterization of heterogeneous conditions, the impact of spatial heterogeneity on power predictions...

  Additional discussion of other wake modeling utilities and the impact of spatial heterogeneity on power prediction accuracy has been added to the introduction. The reader is provided references that offer additional findings related to these topics from Yang et al. (2019) and Clifton and Lundquist (2012) as well.

- About the description of the new implementation, the authors do not mention how they deal with the vertical dimension, especially since they mention in the introduction that a potential application of this new version is wind farms in complex terrains, and the test case is in complex terrains.

  The objective of the proposed methods in this study is to capture heterogeneous atmospheric effects caused by site-specific terrain features, without explicitly modeling the geometry of the wind farm terrain. Therefore, the vertical (z) dimension is not considered when interpolating and extrapolating from the atmospheric inputs. Instead, all input values are assumed to be at the same z location, and the interpolation is performed on a two-dimensional plane at this height. Although this approximation may result in a less accurate result, this approach allows the interpolation and extrapolation algorithm to operate with less computational cost. Additional discussion regarding this issue has been added to the abstract and Section 3.1.

- The part addressing the wind direction heterogeneity and the mesh deformation was not very crystal clear for me and needs more details. Maybe a second case without a constant change in wind direction could be interesting.

  More details addressing the implementation of heterogeneous wind direction in the model has been added to Section 3.3. A second example of non-constant heterogeneous wind direction simulation in an irregularly spaced wind farm has also been included in this section.

- About the test case, the authors could give more information about the wind farm(i.e. number and type of turbines, layout/inter-distance), some information about the complexity of the terrain and about the atmospheric measurements at met masts (temporal evolution of wind speed, wind direction and TI for Days A and B, and some information about the stability).

More information has been added regarding wind farm characteristics. See Section 4, and Appendix A. The chosen wind farm contains several hundred utility-scale wind turbines in location that often is influenced by orographic atmospheric effects. The average stream-wise and span-wise interdistances are 20D and 2D, respectively, where D represents the average rotor diameter of the turbines in this farm.

Specific comments

- P1, L19: you could mention a reference on the "accurate results in uniform set of atmospheric conditions".

  A reference was added to a recent study featuring floris: Fleming et al. (2019)

- P3, L68: you mention "yaw-misalignment conditions" but the $\cos(\gamma)$ is missing in Equation 3. However, as you don't consider any yawing strategy in the paper, maybe you could drop the $\cos(\gamma)$ mentions in all equations. Moreover, u should be infinite velocity or without induction zone.

  $cos(\gamma)$ has been added to Eq. 3.

- In Section 2.3 : you could mention the limitations of the Gaussian model (only valid in far wake)

  - P4, L106: you mention a dependence on ambient TI, but it does not appear until Eq 8. You could mention that this dependence is hidden in k with a reference to Eq 8.

    This has been noted in the text.

  - P4, L114: why do you use quadratic superposition of velocity deficits ? You have an added-TI model and you mention Niayifar and Porté-Agel later: in their paper, they recommend the use of linear superposition of velocity deficit while having an added-TI model.

    Although linear superposition is available as a wake combination method in FLORIS, as discussed in Hamilton et al. (2020), the sum-of-squares method was used in this study because it is a current standard in wake modeling.

– P5, L140: You could nuance this paragraph on turbulence and saturation effect as it is not well understood for now.

This was noted in the text.

– P6, L145: why is the added-TI model part located in the atmospheric stability section ? Moreover, the equation describing the Crespo model is not correct, it should be $0.73a^{0.8325}I_0^{0.0325}(\frac{x}{D})^{-0.32}$. You should also mention the validity ranges ($5 < x/D < 15$, $0.07 < I_0 < 0.014$ and $0.1 < a < 0.4$).

Although the formula you have listed is the correct classic Crespo model, this equation has been 'tuned' from comparisons to higher fidelity models and field study results in Fleming et al. (2020b) and King et al. (2020) to more accurately capture impacts such as secondary steering, deep-wake effects and yaw-induce wake recovery.

- In Section 3:

– P6, L152: You could specify that the heterogeneous flows are undisturbed atmospheric flows (i.e. without wake effects).

This specification has been further emphasized in this section.

– P6, L158: You could make a reference to Fig 1.a.

A reference to Fig. 1a has been added.

– P8, L185: You could name the mentioned algorithms that have been tested for extrapolation, or not mention at all their disadvantages as the explanations are a bit vague and it is difficult to understand what this is about.

More information regarding specific examples have been added. For example, it was found that the analytic continuation of Radial Basis Functions (RBF) and fitted polynomial splines outside of the initial domain often produced a non-feasible output that did not respect the physical limitations of the atmospheric characteristic being extrapolated.

– P8, L203: You could mention a reference to Section 3.3. for the processing of wind direction heterogeneity.

A reference to Section 3.3 has been added to the text.

– P10, Fig 4 and others: You could name turbines (T1 ... T6) and make a reference to T6 in the text.

The turbines have been numbered in Fig. 5a and these numbers have been referenced throughout the text.

– In general for Section 3.3: this procedure with rotation only works if you have uniform lateral change in wind direction ? Maybe you could choose a more complex case for the wind direction change with a bell behaviour or a S-shape. Moreover, how do you define the centre of rotation ? And how do you deal with wake superposition ?

This procedure works with much more complex cases, but a simple case was provided to show the concept in a format that is easy to understand. Figure 9 showing more complex cases has been added. The centre of rotation is defined as the center of the flow field grid, as depicted in Figure 5b. After the velocity deficit behind each wake is calculated, it is subtracted from the free stream velocity of the flow field using the sum-of-squares method described in Katic et al. (1986).

– P10-11, Fig 5 and 6: You could distinguish rotated grid points for single turbine and rotated grid points for all turbines (you have deformation for this grid).

Fig. 6 (formerly Fig. 5) shows the rotated grid points before taking into account the gradual change in wind direction within the simulated flow field. Fig. 7 shows the rotated grid points after the relative changes in wind direction are used to adjust the rotated grid. The rotated gridpoints shown in Fig. 7 are the locations used to calculate the velocity deficit behind turbine T6 in FLORIS. Both Fig. 6 and 7 show stages of the calculation of turbine T6 only. Each turbine wake is calculated independently in its own rotated grid. More details have been added to this section to make this distinction more clear to the reader.

– – In Section 3.4: in this subsection, I can not really say if you deal with heterogeneous ambient/undisturbed TI. It needs some clarification: do you deal with heterogeneous TI the same way you deal with heterogeneous wind speed ? You could add a plot with the corresponding TI in Fig 8.

The implementation of heterogeneous TI and heterogeneous wind speed are similar, in that the initial heterogeneous conditions are established throughout the flow field by interpolating from the input values, and

5

then waked conditions are updated continuously throughout FLORIS computations of flow-field interactions. Calculations for wake propagation use the value of waked turbulence intensity at each turbine, based on the added turbulence model discussed in Section 2.3.2 and Niayifar and Porté-Agel (2015).

– In Section 3.5: Have you used an aero-elastic solver for this part ? You could also give an order of magnitude for Λ.

An aero-elastic solver was not used. Λ cannot have a value equal to or less than zero. This has been noted in Subsection 3.5.

– P14, L276: You could nuance this comment because having an improved Ct should be as important as having an improved Cp as the velocity deficit model relies on Ct.

This comment has been revised in the paper to highlight the benefit of a possible C_T turbulence-correction method implemented for the calculation of velocity deficit.

• In Section 4:

– P14, L281: More information could be given on the wind farm, the layout (min/max inter-distance), the turbines, the complexity of the terrain...

Information regarding the characteristics of the physical layout of the wind farm have been added to Appendix A and Section 4.

– P16, Figure 11/12: You could give more information on the daily evolution of wind speed, wind direction and TI, and on α_s to have an information about stability.

This information cannot be provided because it is confidential. It should be noted that the analysis of Day B was removed because it did not add much to the discussion. This study was primarily focused on improving the power output forecast of conditions that are more variant, and day B was comparatively less variant than day A.

• In Section 5:

– P22, L389: You could give an approximate value of the power prediction improvement.

The percent reduction in mean absolute error for the overall wind farm (14.6% for the heterogeneous model, and 31.42% for the heterogeneous model with turbulence correction) has been added to the conclusion. It should be noted that this improvement factor will vary depending on many circumstances, including the weather patterns and physical layout characteristics a specific wind farm site.

Technical corrections

- In general with the plots on wind direction changes, you could add one or two streamlines, it could help in the understanding.

  White line contours are included on the plots, which help in outlining the wake to increase visibility of flow patterns.

- P5, L134: Consider removing "For simplicity, ky and kz have been set as equal for this model", it has already been mentioned.

  This statement has been removed.

- P6, L174: It should be Fig 1.b and not Fig 1.a.

  This typo has been fixed.

- P7, Fig 1: You could give the title of the colorbox. Is it undisturbed wind speed or wind speed with potential wake effects ?

  To eliminate confusion, Figures 2 and 3 now show an interpolation performed for initial undisturbed wind speed specifically. A label for the colorbar has been added to the figures for reference.

- P7, L194: Consider writing cos and sin not in italics as for arctan2.

  This change has been made.

- P13, Eq 12: d_x should be d_{xi}.

  This change has been made.

- P17, L323: Consider removing one "the".

  This change has been made.

- Tables 1/2: Consider rounding the numbers to integral numbers or with one decimal.

  This change has been made.

- P22, L378: Consider replacing "cause" by "causes".

  This change has been made.

- P22, L390: Consider replacing "show" by "shows".

  This change has been made.

2 Referee 2:

Overall Comment:

The submitted manuscript outlines a modification to the FLORIS package to allow for heterogeneous "freestream" flow conditions at each turbine in the wind farm, i.e. heterogeneous wind speed, direction, and turbulence intensity at each turbine location if no turbines were present. Improving wake models in heterogeneous flow, where wake model assumptions break down, is critical for the design and controls communities, and therefore the subject matter is of relevance to this journal. While this referee recognizes the challenge of formulating consistent engineering models which satisfy key conservation equations, I have some concerns about the derivation of the heterogeneous wake model which should be revisited and articulated by the authors, as this would establish confidence that the newly proposed method could be applied in a general model setting. Further, the test problem shown lacks enough detail to be replicated by readers and must be significantly expanded in detail and in explanation as there are occurrences of model success and failure. Since I believe this model has the potential to be useful to the community, but the manuscript submitted should be modified significantly, I recommend a major revision.

General Comments:

1. This article would greatly improve with a more formal statement of the research objectives. As discussed in the **Specific comments** points, the Abstract and Introduction are full of comments on issues which affect wake model "accuracy." Wake models are fundamentally low-order and are typically derived from first principles with explicit assumptions (uniform 2D or 3D flow chiefly among them). It would be helpful to consider this more carefully.

    (a) Define the objectives of the study and model "accuracy" formally in the introduction. There has to be some degree of baseline performance, since FLORIS cannot be expected to capture power production in strongly complex terrain, for example, since the assumptions made at the stage of derivation break down themselves. Is the hope to capture SCADA power data without resolving any terrain or is the hope to capture realistic flow features (e.g. compare well to LES/WRF in complex terrain)? If the latter is not the goal, how can you demonstrate confidence in the former?

    In developing this proposed model, the objective was to capture a more accurate representation of the effects of wind farm wake interactions within complex terrain, without actually resolving any terrain geometry during simulation. This study analyzes the heterogeneous model's accuracy in power output prediction as a measure of FLORIS mod-

eling performance. Additional discussion regarding the objectives of this study have been added to the introduction.

(b) Discuss previous studies which have highlighted issues with uniform inflow formulations and how this study specifically addresses those issues. I recommend expanding the literature review.

Further discussion of literature that investigates this issue (such as Yang et al. (2019)) has been added to the introduction.

(c) Three previous heterogeneous models are discussed, why are those methodologies not employed or inaccurate such that this study is necessary?

The other heterogeneous models were mentioned in this paper to acknowledge their efforts in the body of research related to this issue of spatial heterogeneity within wind farms in complex terrain. Each of these referenced models present valid and useful findings, but their methods were not employed in this study because a potential for success was also identified using the approach of the proposed model. This study was conducted to specifically analyze the effectiveness of the proposed approach to modeling spatially heterogeneous flow.

2. Problematically, the proposed method does conserve momentum and gives different values of turbine thrust depending on the size of the control volume drawn around the turbine in complex flow (see discussion below). Many engineering models do not conserve key quantities, but it is important to derive consistent models from first principles otherwise we will not know when the core assumptions are valid or invalid in a new wind farm or model situation.

These issues have been addressed in the paper and in the relevant **Specific comments** *below.*

3. The new methods would benefit from a validation case of the methods (e.g. a comparison to complex flow RANS/LES rather than just comparing power predictions for one wind farm). It's hard to extrapolate that marginally improved power production modeling for one wind farm generalizes to claim that the newly developed model is an improvement given all of the uncertainties associated with low-order wake models and empirical considerations detailed in the **Specific comments** below.

In another recent study (Fleming et al., 2020a), simulations from the

*proposed heterogeneous FLORIS model are compared to LES results for a case study of a 38-turbine wind farm. The analysis showed that including spatially heterogeneous wind speed lowers the error in predictions of total power production by 15% in comparison to the homogeneous solution. Further comments regarding validations in this study have been addressed in relevant **Specific comments** below.*

4. There are a significant number of questions/issues with the results section of this manuscript. I have detailed them below in the **Specific Comments**. If the authors can address these comments the manuscript would greatly improve. Very little information/data is given about the test case and even in this limited test scenario the model 'improvement' is not convincing since it does not outperform homogeneous FLORIS for all cases and there is no explanation given for the varying degrees of success.

   *These issues have been addressed in the relevant **Specific comments** below.*

2.1   Specific comments:

1. Line 5: The abstract should briefly mention the hypothesized causes of heterogenous wind flow. It is not clear to this referee just by reading the abstract the focus of the heterogenous model. Specifically, is this paper addressing heterogeneity due to: 1) site-specific complex terrain, 2) short-time averaging of quasi-homogeneous turbulent flow, 3) wake heterogeneity, 4) etc. This should be stated concisely in the abstract.

   The objective of the proposed methods is to capture heterogeneous atmospheric effects caused by site-specific terrain features, without explicitly modeling the geometry of the wind farm terrain. This has been mentioned in the abstract.

2. Line 10: The abstract should explicitly state the key results of the paper. For example, was the new heterogeneous extension to FLORIS successful in the figures of merit of focus for the present study?

   Information regarding this model's performance has been added to the abstract.

3. Introduction:

   (a) The introduction is very brief and can be improved as discussed in **General comments.**

11

See responses to No. 1 in **General Comments.**

(b) This introduction assumes significant familiarity with FLORIS. That would be acceptable in a conference paper but not for a journal article, which should be self-contained. For example, the concept of "steady state" time-averaging in the FLORIS name isn't even introduced.

Additional information regarding the concept of "steady state" time-averaging and other general details about FLORIS have been added to Section 2. The reader is also given several sources to expand further background research on the basic concepts involving FLORIS operation.

(c) The introduction should cover wake models more broadly rather than only FLORIS, since this paper is attempting to develop new heterogeneous wake model capabilities for the literature.

Additional references to other wake models has been added to the introduction.

4. Equation 1: Define the axial induction factor

A definition of the axial induction factor has been added.

5. Line 95: Since this article details modifications to the flow calculation within FLORIS, the authors should explicitly detail all of the assumptions within the derivation of the Gaussian wake model to ensure consistency between the analytical wake model formulation and the freestream condition specification in this implementation of FLORIS. For example, the Guassian wake model (Bastankhah & Porte-Agel (2014)) assumes zero pressure gradients which is then violated in the heterogeneous model.

Additional discussion relating to the assumptions within the derivation of the Gaussian wake model, and the ways in which the heterogeneous methods may violate these assumptions have added in Section 2.3.1

6. Equation 7: The current proposed method of heterogeneous wind speed, should the local shear coefficient also be modified?

In this study, the shear coefficient was assumed to be homogeneous throughout the flow field. FLORIS currently does not have functionality to define

a spatially heterogeneous shear coefficient. In future work, the benefit of this functionality may be investigated for improvement of the model.

7. Equation 8: How are ka and kb affected by complex terrain since the empirical fit to idealized LES calculations performed by Niayifar and Porte Agel assume no terrain

   In Fleming et al. (2020b), the results of a field study analysis focusing on the performance of these tuned parameters is presented, comparing two campaigns located in comparatively simple and complex terrains. The results of this study show a trend of possible underprediction of wake losses in areas with complex terrain due to the influence of several tuning parameters. Since the same default values for k_a and k_b are used in Fleming et al. (2020b) as in this study, it provides a very relevant analysis of the fit of these terms.

8. Equation 8: It is very unlikely that ky= kz in complex terrain. Please perform a sensitivity analysis of the results on this assumption.

   Based on the defined relationship between k_y/k_z and k_a/k_b, it would be reasonable to assume that the effects that complex terrain have on k_y and k_z will be similar to those observed for k_a and k_b in Fleming et al. (2020b).

9. Equation 10: This equation was also empirically tuned for homogeneous flow and simple terrain and a sensitivity analysis on these parameters must be investigated.

   The findings from Fleming et al. (2020b) indicate that there may be a slightly worsened effect of FLORIS's tendency to underpredict wake losses in areas with complex terrain using this equation. These effects have been noted in this section of the paper, and the parameters in this equation have also been updated to reflect the most recent tunings found in FLORIS currently.

10. Section 3.1 would benefit from a pseudo-code/diagram to improve reader understanding

    A psuedo-code diagram has been added to explain the steps involved in initializing the flow field. See Fig. 1.

11. Line 185: The explanation of the selection of interpolation algorithms is insufficient.

(a) What is the justification of linear Barycentric interpolation? Likely the validity of linear interpolation depends on the complexity of the underlying terrain and should be discussed in more detail.

Linear Barycentric interpolation was chosen because it is relatively simple in computation and can be easily implemented without requiring any input parameters other than the locations and values of wind measurements. It is correct that the accuracy of the interpolated values is dependent on the input measurements provided, and the complexity of the weather patterns in the physical wind farm. Additional information regarding this issue has been added to Section 3.1.

(b) Detailed comparisons for the extrapolation should be shown in the Appendix and not just mentioned briefly, since often sensors are not widely available at wind farm sites (usually only a few MET towers for many tens of turbines). Therefore, the performance of the extrapolation will likely be critical to model success.

For this test case, it is difficult to compare the accuracy of extrapolated wind measurements, because there is little data available that shows the actual atmospheric behavior at the wind farm during the time span of this study, other than the MET masts used for inputs for the FLORIS simulations. The heterogeneous model is not able to introduce precise details of initial flow-field conditions beyond the bounds of the measurements taken from the wind farm, but this is not the goal of the extrapolation processes. These extrapolations within the heterogeneous model aim to represent an approximation of the observed conditions, based on the limited wind measurements provided.

12. Line 200: The 3D velocity field calculation with the power law assumes that the MET towers are in the same vertical location (z) (otherwise the Barycentric interpolation would not be possible I believe). Often MET masts have varying heights, and this may be of interest to consider for the authors.

In this study, all input measurement locations were assumed to be at the same vertical location (z) for simplicity. In future work, it may be beneficial to add the functionality of varying input measurements to FLORIS, given that MET towers are typically located at varying heights in real wind farms.

13. Figures 1 and 2: What is the color axis representing in the sketch?

For clarity, Fig. 1 and 2 (now Fig. 2 and 3) now indicate the interpolation

performed for wind speed, in meters per second. A label for the colorbar has been added to the figures for reference.

14. Line 204: What is u used by the sum-of-squares velocity deficit in the local velocity u_∞ calculation in heterogeneous flow?

    The value of U_∞ used in the deficit calculation for $u(x, y, z)$ in Eq. 4 is equal to U_{init}, which is calculated using the power-log law of wind (Eq. 7).

15. Line 204: **Please state the equation for the velocity deficit update explicitly.** For the purpose of this review, I will assume it is as stated below, although if the formulation is different then this discussion may not apply. I assume that this is the formulation also because Figure 6 has a velocity deficit axis which becomes negative. $u(x, y, z) = U_{init} * (1 - C[exp(-(y-\delta)^2/2\sigma_y)exp(z-z_h)^2/2\sigma_z)$ where C is a function of the upwind turbine's C_T which is a function of the average velocity of the upwind turbine U_{upwind}. The velocity deficit calculation is not consistent with actuator disk theory since $U_{upwind} \neq U_{init}$. The velocity deficit trailing a wind turbine ($u(x, y, z)$ in Equation (4)) is a function of C_T and U_{upwind}. The local calculation here specifies that the velocity deficit trailing a turbine is a function of the turbine thrust coefficient (which is based on the average velocity of the upwind turbine) and the *downwind velocity*.

    The equation for velocity deficit that is stated above is the one used in the proposed model. Section 2.2 has been revised so that this equation is explicitly stated.

    (a) Illustrative example: A turbine generates a velocity deficit $u_1(x, y, z)$ in a uniform flow field. If in complex terrain, there was a local flow acceleration due to a hill downwind of the turbine, that means the velocity deficit will also increase.

    (b) This formulation means that the turbine thrust is not a fixed quantity but depends on the downwind position (since U_{init} is a function of x) and therefore momentum is not conserved (as shown by a control volume analysis). Heterogeneities in U_{init} arise from pressure gradients which are neglected in the Gaussian wake model and FLORIS.

    (c) Perhaps the authors have only used U_{init} in the sum-of-squares calculation?

        U_{init} has been used in the velocity deficit calculations, and in the sum-of-squares calculations. This means that the proposed heterogeneous violates the principle of momentum conservation, according to this control-volume analysis. This has been noted in the paper.

(d) The authors should consider Brogna et al. "A new wake model and comparison of eight algorithms for layout optimization of wind farms in complex terrain" (2020) which proposes a modified Gaussian wake model in complex terrain where the spatial U_∞ evolution is considered in the superposition but not in the velocity deficit calculation aside from modifying the turbine specific C_T.

In future developments, the benefits of an approach similar to this may be investigated to improve overall momentum conservation in the FLORIS model. This has been mentioned in the paper and the relevant article cited.

16. Figure 3: No details of the domain geometry, turbines, etc are shown for this figure and it will be very hard to reproduce. It is unclear to this referee what this figure adds, since it shows different velocity colors but it is unclear whether these heterogeneous speeds are valid/correct with no underlying baseline solution (e.g. from complex terrain LES or LiDAR).

Fig. 3 (now Fig. 4) provides an exemplary hypothetical case to show how the heterogeneous effects of the model can be observed visually as an additional method of analysis. These plots have not been compared to LES or LiDAR solutions.

17. Figure 5: The colormap is confusing or incorrect since the velocity deficit values are not computed

The velocity deficit colorbar has been removed from this figure for clarity.

18. Line 215: Are the 3D velocity deficits (due to the changing inflow angle) included in the local wind direction computation of downwind turbines?

The velocity deficit of upwind turbines does not affect the local wind direction at a downwind turbine. The wind direction at all points in the flow field are interpolated from the initial inputs when the flow field is initialized. After flow field initialization, the wind direction values are not changed during wake calculations, unless the flow field is re-initialized with differing wind direction inputs.

19. Line 225: More discussion of the sensitivity to grid spacing is warranted. What were the authors' methodology for changing the grid spacing in the y-direction?

As discussed in Section 3.4, the changes in the grid spacing in the y-direction are dependent on the varying gradient of wind direction within the flow field. Without this variation, the FLORIS model would only be able to define a single wind direction for each turbine, and not a gradual change throughout the flow domain.

20. Line 230: The current model does not resolve the momentum source/sinks from the complex terrain and therefore does not satisfy momentum conservation even with a fixed spacing in the y-direction.

    This is an important concept to consider in this proposed model, and has been noted in the paper. In the heterogeneous model, the wind farm's physical terrain is not modeled, and the effects of this terrain are approximated to the heterogeneous wind measurements used as inputs. Although this method does not conserve momentum, the approximations imposed in the model prove to be effective in modeling the effects of the landscape, based on the results of this study.

21. Line 240: What is the limiting case of wind direction changes that this model can accept?

    The limiting case of wind direction change is that which causes the flow-field grid points to overlap themselves in the process of rotation during velocity deficit calculations, as shown in Fig. 6 and 7. This limit is determined for each farm independently and varies with the site-specific layout geometry of each case. This has also been further elaborated on in Section 3.3.

22. Line 255: The discussion of turbulence intensity's influence on the power curve deserves some literature review, as this has been studied previously (e.g. "Accounting for the effect of turbulence on wind turbine power curves" Clifton & Wagner TORQUE 2014).

    The proposed method of accounting for turbulence intensity power effects was developed with the goal of operating without a dependency on the availability of training data or empirical values for this study. In future work, it may be advantageous to incorporate more complex techniques that are able to capture the effects of turbulence intensity with greater detail and accuracy. More information regarding this issue has been added to Section 3.5 of the paper.

23. Figure 10: From this figure, the wake losses look very insignificant due to large streamwise spacing. What would be the power production predic-

tion if the wake model was not used and the power of each turbine was computed only using U_{init} ?

Information regarding the relative size and geometry of the wind farm layout and turbines has been added to Appendix A. This should give an indication of the influence of wake effects at this site. Identical simulations were also performed with the omission of wake calculations to evaluate the significance of wake losses for this study. See relevant tables in Appendix B.

24. Section 4:

   (a) The terrain map should be shown given that this paper aims to represent heterogeneity associated with complex terrain/wind flow conditions

   The exact terrain map for this study cannot be given because it is proprietary, although the relevant characteristics of the terrain geometry have been added to the Appendix.

   (b) More details on the SCADA data processing should be given in the Appendix,and ideally, the data would be provided to ensure reproducibility of the results. If the SCADA data must be kept confidential, another test case (with data) must be provided in this paper to ensure reproducibility of results.

   Unfortunately, the SCADA data is confidential for this wind farm. A second wind farm with similar terrain characteristics and operational conditions could not be found to perform a second simulation, due to the common industry practice of making commercial wind farm SCADA data confidential.

   (c) Why was a timestep of 30 minutes chosen for the FLORIS model runs? Have the authors performed a sensitivity analysis on that timescale selection?

   In preliminary time scale sensitivity analyses, it was observed that time steps that were of a longer duration typically had a lower accuracy in power predictions throughout all three FLORIS models.30 minute time steps were originally chosen for this study because they are frequent enough to show substantial exemplification of the added power prediction accuracy offered by the proposed model, while still maintaining a moderate computational expense in simulation. In the recently updated results of this study, the simulations were performed

at 10 minute time steps to provide an even more detailed analysis of this model, and to meet the common standards of the industry.

(d) Figure 10: The axes are not labeled with the physical coordinates, so the advection time scale of the wind farm cannot be estimated and the results will not be reproducible.

The exact coordinates of the wind farm cannot be given, because this information is confidential, but details that give the relative geometry of the wind farm have been added to the Appendix.

(e) Figures 11 and 12: What do the authors refer to as "atmospheric variations?" Figures of the wind speeds, directions, turbulence intensity, etc. should be included for the MET towers, at least in an Appendix.

The "atmospheric variations" discussed in these figures refer to changes in wind direction, wind speed, and turbulence intensity in each given day. This information cannot be included because it is confidential. It should also be noted that the analysis of Day B was removed because it did not add much to the discussion of model performance. This study was primarily focused on improving the power output forecast of conditions that are more variant, and day B was comparatively less variant than day A.

(f) Figures 11 and 12: What has the power been normalized by? No details are given on the normalization strategy.

The power has been normalized by the rated output for the subject wind farm. This is now noted in the paper.

(g) Figure 15: For context, please include a vertical line for each of the cases showing the mean percent error over the datasets overlaid on the histograms.

Vertical lines have been added to the figures.

(h) The wind farm power production per turbine should be included as well. This paper gives no indication of the wake losses at the site.

Table 3 has been added to show the average error from all of the individual turbines of the wind farm. Additional information regarding the relative geometry of the subject wind farm has also been appended to give a better indication of the wake losses at the site.

19

(i) Table 1

    i. The heterogeneous model outperforms the homogeneous case when the wind speed is larger (>11 m/s) and there are small wake losses.

    ii. The model also outperforms homogeneous within 5-11 m/s where wake losses are present.

    iii. The authors do not give a clear explanation as to why the model performs poorly in low wind speed (when I assume heterogeneity is more significant at the site but I cannot deduce this from data since that data has not been shown). The authors instead show the results in a different metric and claim success. It would be much more valuable for the community to understand and explain why the new heterogeneous model correction sometimes is good and sometimes is bad at this particular site.

As discussed in Section 4, this may be due to the inherent "bias" of the metric of Mean Average Percent Error (MAPE), which penalizes overpredictions with more weight than underpredictions. In comparison to the metric Mean Absolute Error (MAE), MAPE also shows an equally weighted mean error regardless of the overall power output per time step, which is often times not preferred for an indication of overall farm power output accuracy. It is possible that the reported increase in MAPE with lower wind speeds may be an indication that the heterogeneous and turbulence intensity correction models tend to produce more frequent overpredictions of power output in conditions where wind speeds are near the cut-in speed.

If this is true, it may indicate that the proposed interpolation methods have a tendency to define disproportionately high velocity values (U_{init}) at flow-field points in predominantly low-velocity settings, causing an overestimate of power production as a result. In future work, this could be circumvented by implementing more complex interpolation strategies that consider the physical dynamics of changing velocity in naturally occurring fluid flow.

Technical corrections:

1. Title: It would be more precise for the title of this manuscript to be "Design and analysis of a wake model for spatially heterogeneous flow"

The title has been changed.

2. Line 90: Period typo.

This typo has been fixed.

References

Clifton, A. and Lundquist, J. K.: Data Clustering Reveals Climate Impacts on Local Wind Phenomena, Journal of Applied Meteorology and Climatology, 51, 1547–1557, https://doi.org/10.1175/JAMC-D-11-0227.1, URL `https://doi.org/10.1175/JAMC-D-11-0227.1`, 2012.

Fleming, P., King, J., Dykes, K., Simley, E., Roadman, J., Scholbrock, A., Murphy, P., Lundquist, J. K., Moriarty, P., Fleming, K., van Dam, J., Bay, C., Mudafort, R., Lopez, H., Skopek, J., Scott, M., Ryan, B., Guernsey, C., and Brake, D.: Initial results from a field campaign of wake steering applied at a commercialwind farm – Part 1, Wind Energy Science, 4, 273–285, https://doi.org/10.5194/wes-4-273-2019, URL `https://www.wind-energ-sci.net/4/273/2019/`, 2019.

Fleming, P., King, J., Bay, C. J., Simley, E., Mudafort, R., Hamilton, N., Farrell, A., and Martinez-Tossas, L.: Overview of FLORIS updates, Journal of Physics: Conference Series, 1618, 022 028, https://doi.org/10.1088/1742-6596/1618/2/022028, URL `https://doi.org/10.1088/1742-6596/1618/2/022028`, 2020a.

Fleming, P., King, J., Simley, E., Roadman, J., Scholbrock, A., Murphy, P., Lundquist, J. K., Moriarty, P., Fleming, K., van Dam, J., Bay, C., Mudafort, R., Jager, D., Skopek, J., Scott, M., Ryan, B., Guernsey, C., and Brake, D.: Continued results from a field campaign of wake steering applied at a commercial wind farm – Part 2, Wind Energy Science, 5, 945–958, https://doi.org/10.5194/wes-5-945-2020, URL `https://wes.copernicus.org/articles/5/945/2020/`, 2020b.

Hamilton, N., Bay, C. J., Fleming, P., King, J., and Martínez-Tossas, L. A.: Comparison of modular analytical wake models to the Lillgrund wind plant, Journal of Renewable and Sustainable Energy, 12, 053 311, https://doi.org/10.1063/5.0018695, URL `https://doi.org/10.1063/5.0018695`, 2020.

Katic, I., Højstrup, J., and Jensen, N. O.: A simple model for cluster efficiency, in: European wind energy association conference and exhibition, pp. 407–410, 1986.

King, J., Fleming, P., King, R., Martínez-Tossas, L. A., Bay, C. J., Mudafort, R., and Simley, E.: Controls-Oriented Model for Secondary Effects of Wake Steering, Wind Energy Science Discussions, 2020, 1–22, https://doi.org/10.5194/wes-2020-3, URL `https://wes.copernicus.org/preprints/wes-2020-3/`, 2020.

Niayifar, A. and Porté-Agel, F.: A new analytical model for wind farm power prediction, Journal of Physics: Conference Series, 625, 012 039, https://doi.org/10.1088/1742-6596/625/1/012039, 2015.

Yang, M., Zhang, L., Cui, Y., Yang, Q., and Huang, B.: The impact of wind field spatial heterogeneity and variability on short-term wind power forecast errors, Journal of Renewable and Sustainable Energy, 11, 033 304, https://doi.org/10.1063/1.5064438, 2019.

Design and analysis of a <u>wake model for</u> spatially heterogeneous <u>~~wake~~</u><u>flow</u>

Alayna Farrell[1], Jennifer King[1], Caroline Draxl[1], Rafael Mudafort[1], Nicholas Hamilton[1], Christopher J. Bay[1], Paul Fleming[1], and Eric Simley[1]

[1]National Renewable Energy Laboratory, Golden, CO, 80401, USA

Correspondence: afarrell@msu.edu, floris@nrel.gov

Abstract. Methods of turbine wake modeling are being developed to more accurately account for spatially variant atmospheric conditions within wind farms. Most current wake modeling utilities are designed to apply a uniform flow field to the entire domain of a wind farm. When this method is used, the accuracy of power prediction and wind farm controls can be compromised depending on the flow-field characteristics of a particular area. In an effort to improve strategies of wind farm wake modeling and power prediction, FLOw Redirection and Induction in Steady State (FLORIS) was developed to implement sophisticated methods of atmospheric characterization and power output calculation. In this paper, we describe an adapted FLORIS model that features spatial heterogeneity in flow-field characterization. This model approximates an observed flow field by interpolating from a set of atmospheric measurements that represent local weather conditions. The <u>objective of this method is to capture heterogeneous atmospheric effects caused by site-specific terrain features, without explicitly modeling the geometry of the wind farm terrain. The implemented</u> adaptations were validated by comparing the simulated power predictions generated from FLORIS to the actual recorded wind farm output from the Supervisory Control And Data Acquisition (SCADA) recordings. <u>In the results of these validation analyses, the FLORIS simulations that implemented the heterogeneous flow model showed a 14.6% decrease in Mean Absolute Error (MAE) of wind farm power output prediction, in comparison to the original homogeneous model simulations.</u> This work quantifies the accuracy of wind plant power predictions under heterogeneous flow conditions and establishes best practices for atmospheric surveying for wake modeling.

1 Introduction

Low-fidelity wake modeling utilities such as FLOw Redirection and Induction in Steady State (FLORIS) are typically used for the estimation of wind farm power output or the implementation of wind farm controls that help improve the overall performance of a wind farm. This includes implementing real-time corrective strategies that aid in reducing stress-inducing loads on turbines (Boersma et al., 2017), avoiding operational side effects like noise pollution (Leloudas et al., 2007) or shadow flicker (Clarke, 1991), and maximizing power output through methods of wake steering and power grid optimization (Fleming et al., 2017b). FLORIS, and most other controls-oriented wake modeling utilities, implement advanced wake modeling algorithms that are capable of producing accurate results in a uniform set of atmospheric conditions <u>(Fleming et al., 2019)</u>. However, the accuracy of any wake model is highly dependent on its ability to recreate the characteristics present. It is important for these

25 models to be able to emulate the naturally occurring state of the wind farm as closely as possible for the controls processes and power-prediction functionalities to operate with reliable accuracy. Most current controls-oriented wake modeling utilities use a homogeneous approximation to characterize the initial state of the atmosphere. Requiring a homogeneous flow is a limitation in most engineering wake models. Error correction terms are proposed in Schreiber et al. (2019), where these correction terms are learned from operational data.

30 The consequences are particularly evident when observing the accuracy of power predictions for wind farms located within complex terrain, or wind farms that are otherwise subject to highly variant conditions in the atmosphere. Because these atmospheres are subject to dramatic changes in the velocity and direction of wind, it is difficult to anticipate how the resulting wakes will form and what kind of power output should be expected. ~~With this uncertainty~~ In Yang et al. (2019), an analysis of the impact of spatial heterogeneity in wind farm flow is presented for a site within complex terrain. It showed that using averaged

35 values of wind conditions caused short-term wind power forecasting to be less accurate, due to spatial heterogeneity within the wind field and the variability of wind turbine power curves. With these effects considered, the current version of FLORIS and many other wake model utilities are not constructed to accurately model fluid flow during these conditions. It should be noted that there are existing wake models that incorporate elements of heterogeneous wake effects caused by varying atmospheric conditions. For example, one model presented in You et al. (2016) takes a statistical approach in representing heterogeneous

40 power deficit caused by wind farm-flow interactions in variant weather conditions. Another method discussed in Shao et al. (2019) proposes an interaction model used for calculating the turbulence intensity of overlapping wakes, and represents the relative positions of wind turbines under arbitrary and variant wind direction conditions. Clustering methods have also been implemented, such as Katic et al. (1986) and Clifton and Lundquist (2012), where the turbines of a wind farm are sectioned into groups, assigning a differing atmospheric characteristic to each cluster of turbines to mimic the heterogeneous conditions

45 observed in natural atmospheres.

The aforementioned models present many methods for approximating farm-flow interaction in heterogeneous conditions. As a contribution to this area of research, this article will present a modified version of FLORIS that features an advantageous capability in modeling wind farms with variant weather conditions and complex terrain. This adapted version of FLORIS presents several novel developments within the scope of controls-oriented wake modeling research: an interpolation algorithm

50 is implemented, which allows the user to define a gradient of atmospheric characteristics across the flow field, based on several measurements within or adjacent to the wind farm; elements of spatially variant wind direction, wind speed, and turbulence intensity are integrated into wake calculations of the preexisting FLORIS model; and an additional method is introduced to minimize error in power-prediction accuracy caused from high-turbulence intensity and wind speed variance. ~~To validate these methods, this article evaluates the performance of the developed FLORIS modelby analyzing its~~

55 In developing this proposed model, the objective was to capture a more accurate representation of the effects of wind farm wake interactions within complex terrain, without actually resolving any terrain geometry during simulation. This study analyzes the heterogeneous model's accuracy in power ~~prediction.~~ output prediction as a measure of wake effect modeling performance. In future studies, the authors would like to compare results of this developed FLORIS model to RANS/LES to derive more detailed evaluation of the proposed model's capabilities.

2 Existing FLORIS model

FLORIS (NREL, 2019) is a wake modeling utility that is equipped with tools designed for the control and optimization of wind farms, and is being developed at the National Renewable Energy Laboratory (NREL) in collaboration with Delft University of Technology. This tool uses several computational modeling techniques ~~,~~ paired with controls algorithms ~~,~~ to approximate and optimize wind turbine wake interactions through integration of real-time supervisory control and data acquisition (SCADA) data recorded from wind farms. ~~It also can~~ FLORIS implements the concept of steady-state averaging to simulate the observed dynamic behavior within a wind farm for each iteration in time, and can also be used as a simulation tool to compute farm-flow ~~interaction~~ interactions in wind farms under user-defined atmospheric conditions. This section will give an overview of the mathematical theory in which the formulations of the wake models of FLORIS were based. These concepts are also explained in greater detail in Annoni et al. (2018) and Hamilton et al. (2020).

2.1 Turbine power-output model

The operation and performance of a turbine is modeled with respect to the relationship between the thrust coefficient, C_T, and power coefficient, C_P. The dependence between these two terms characterizes a turbine's power output and wake propagation, therefore making the understanding of this relationship fundamental to the design and operation of wind farm controls. To model the performance behaviors of a given turbine, a table is constructed inside of FLORIS that tabulates C_T and C_P with respect to wind speed. This table can be set to a user's self-obtained data, generated independently by NREL's FAST (Jonkman, 2010), or by integrating CCBlade (Ning, 2013) with FLORIS. The relationship between C_T and C_P can also be defined through the concept of actuator disk theory~~, where~~. This theory relates the turbine power output and thrust ~~are linked~~ through the axial induction factor, a~~:~~, which can be calculated using the definitions from Burton et al. (2002) and Bastankhah and Porté-Agel (2016):

$$C_P = 4a(1-a)^2 \tag{1}$$

$$C_T = 4a(1-a) \tag{2}$$

From these values, the power can then be calculated for turbines under steady-state and yaw-misalignment conditions, using the following relationship provided by Burton et al. (2002):

$$P = \frac{1}{2}\rho A C_P u^3 cos\gamma^p \tag{3}$$

where ρ is the air density, A is the rotor-swept area, ~~and~~ u is the rotor-averaged wind speed~~.~~

, and p is a tuneable parameter that accounts for the power losses due to yaw misalignment seen in simulations (Burton et al., 2002; Fleming et al., 2017a). Thus far, the turbine model discussed in this section does not consider the effects that turbulence may have on the relationship between power output and wind speed. However, Sheinman and Rosen (1992) analyze the effects of turbulence intensity on wind farm power output. In this study, it is shown that turbine power output can

be overestimated by more than 10% if turbulence intensity is not considered. Many empirical and machine-learning methods have been proposed to solve this issue. However, a nonparametric statistical averaging model may be preferred, such as the model developed in Hedevang (2014). In Section 3.5, a new method of implementing a turbulence-dependent correction to power will be discussed for FLORIS applications.

2.2 Velocity deficit

FLORIS provides an option to select particular models for wake velocity deficit and wake deflection separately to suit the user's performance needs. The variety in modeling capabilities reflects a range of trade-offs between computational efficiency and the number of detailed physics applications applied to calculations. If a model is more computationally expensive, it is likely to implement more sophisticated algorithms as well, in hopes of achieving a more accurate result. These models all have a different approach to modeling turbine wake interactions, and offer different strengths and weaknesses in functionality. Most models can either be classified as a velocity deficit, or a wake deflection calculation, but there are also the Gaussian and Curl models that incorporate both calculations and extend further into the overall FLORIS wake modeling structure and control tools. For the purposes of this article, only the Gaussian wake model will be explained in-depth. See Annoni et al. (2018), Martínez-Tossas et al. (2019), and Bay et al. (2019) for details on additional models in FLORIS.

2.3 Gaussian wake

The Gaussian Wake Model is comprised from a series of papers, including Bastankhah and Porté-Agel (2014); Abkar and Porté-Agel (2015); Niayifar and Porté-Agel (2015); Bastankhah and Porté-Agel (2016); Dilip and Porté-Agel (2017). This model is a method of calculation that is integrated into the structure of all FLORIS wake modeling and control tools. It integrates the concepts of the Bastankhah and Porté-Agel wake deflection model, the self-similar velocity deficit model, and elements of atmospheric stability into one comprehensive method based off of the concept of a Gaussian wake (Pope, 2000). This section will describe the different concepts that are implemented in this model.

2.3.1 Self-Similar Velocity Deficit

The Gaussian model computes the streamwise velocity deficit at any point in a turbine's wake by using analytical formulations of Reynolds-averaged Navier-Stokes (RANS) equations to an assumed Gaussian wake profile. The Gaussian wake is based on the self-similarity theory used for free shear flows (Pope, 2000), and is developed under the assumption of no pressure gradients within the initial undisturbed free-stream flow and uniform flat terrain (Bastankhah and Porté-Agel, 2014). To calculate the

velocity deficit, $u(x,y,z)$, behind the rotor of a turbine:

$$u(x,y,z) = U_\infty \left(1 - C \left[exp\left(-\left(y-\delta\right)^2/2\sigma_y^2 \right) \cdot exp\left(-\left(z-z_h\right)^2/2\sigma_z^2 \right) \right] \right) \tag{4}$$

$$C = 1 - \sqrt{1 - \frac{(\sigma_{y0}\sigma_{z0})C_0(2-C_0)}{\sigma_y \sigma_z}}$$

$$C_0 = 1 - \sqrt{1 - C_T},$$

where U_∞ is the freestream velocity; $x, y,$ and z represent the spatial coordinates in the streamwise, spanwise, and vertical directions, respectively; and z_h is the turbine hub height. C is the velocity deficit at the wake center; δ represents the wake deflection computed with equations from Bastankhah and Porté-Agel (2016); and σ denotes the wake width in the lateral (y), and vertical (z) directions. The subscript "0" references a term's initial value at the start of the far wake.

The wake width in the y and z directions, σ_y and σ_z, are determined by the thrust coefficient, C_T, and the wake expansion rate, which is parameterized by k_y and k_z:

$$\frac{\sigma_z}{D} = k_z \frac{(x-x_0)}{D} + \frac{\sigma_{z0}}{D}, \quad \text{where} \quad \frac{\sigma_{z0}}{D} = \frac{1}{2}\sqrt{\frac{u_R}{U_\infty + u_0}}, \tag{5}$$

$$\frac{\sigma_y}{D} = k_y \frac{(x-x_0)}{D} + \frac{\sigma_{y0}}{D}, \quad \text{where} \quad \frac{\sigma_{y0}}{D} = \frac{\sigma_{z0}}{D}\cos\gamma, \tag{6}$$

where D is the rotor diameter, u_R is the velocity at the rotor, γ denotes the turbine's yaw offset, and u_0 represents the maximum velocity deficit in the wake. Parameters k_y and k_z are dependent on the value the ambient turbulence intensity, I_0, as noted in Eq. 8.

The findings of Abkar and Porté-Agel (2015) demonstrate that k_y and k_z grow at different rates, but in order to simplify the model, k_y and k_z are usually set as equal. The total velocity deficit at any point in the domain of fluid flow can then be calculated by combining the wakes using the sum-of-squares method described in Katic et al. (1986).

In the scope of this study, it is important to note that the introduction of spatial heterogeneity in initial wind conditions (which is a key principle in the proposed model) violates the original assumption of no pressure gradient for the derivation of the Gaussian wake model. Although this limits the model's ability to conserve key principles that govern the physical dynamics of fluid flow, the results of this study show that the measured improvements in model accuracy outweigh the consequences of incomplete conservation. In Brogna et al. (2020), a modified Gaussian wake model is implemented to simulate wind farms in complex terrain, but the spatial U_∞ evolution is considered only in the superposition of wakes and is omitted for the calculation of the velocity itself. The benefits of an approach similar to this could be investigated in future FLORIS developments to improve overall momentum conservation for the heterogeneous model.

2.3.2 Atmospheric Stability

The Gaussian model also implements methods proposed by Abkar and Porté-Agel (2015); Niayifar and Porté-Agel (2015), which characterize the effects of atmospheric stability by analyzing the levels of veer, shear, and changes to turbulence intensity in the fluid flow. Stull (2012) discusses that an accurate representation of atmospheric stability requires the measurement of many other variables in the atmosphere; but without detailed recordings of elements such as temperature profiles and vertical flux, the three chosen parameters are able to give a rough idea of the state of the atmosphere in the FLORIS model.

To implement the effects of shear, α_s, the power-log law of wind is used to define the initial wind speed in the flow field, U_{init}:

$$\frac{U_{\text{init}}}{U_\infty} = \left(\frac{z}{z_h}\right)^{\alpha_s}, \tag{7}$$

where a high shear coefficient ($\alpha_s > 0.2$) is indicative of stable atmospheric conditions, and a low shear coefficient ($\alpha_s < 0.2$) characterizes an unstable atmosphere (Stull, 2012).

The Gaussian model was designed to avoid the inaccuracies caused by neglecting the effects of turbulence intensity by implementing methods introduced by Niayifar and Porté-Agel (2015). This also includes added turbulence caused by nearby turbine operation to more accurately calculate the rate of wake expansion. Many other linear-flow models use a constant parameter that defines the rate of wake expansion and has no dependency on the operating conditions of the turbine (Jensen (1983)). From the concepts of Niayifar and Porté-Agel (2015), the Gaussian model relates the rate of wake expansion in the lateral and vertical directions directly to the ambient turbulence intensity present at a turbine and two tuned parameters, $k_a = 0.38371$ and $k_b = 0.003678$:

$$k_y = k_z = k_a I + k_b. \tag{8}$$

For simplicity, k_y and k_z have been set as equal for this model.

The turbulence intensity, I, is calculated by superimposing the initial ambient turbulence intensity (I_0) with the sum of the added turbulence caused by the operation of each influencing upstream turbine, j and I_j^+. The following relationship is used in FLORIS to calculate the ambient turbulence intensity at a given turbine with respect to neighboring turbine wakes:

$$I = \sqrt{\sum_{j=0}^{N} \left(I_j^+\right)^2 + I_0^2}. \tag{9}$$

N refers to the number of upstream turbines that create a wake that adds to the ambient turbulence intensity at a downstream turbine's location. In Niayifar and Porté-Agel (2015), this number was assumed to be one, and the closest turbine was only taken into account because it would theoretically give the maximum amount of added turbulence. In the Gaussian model used in FLORIS, all turbines within a distance of $15D$ upstream and $2D$ in the ~~spanwize~~ span-wise (y) direction are included. ~~This~~

170 Although the saturation effects of turbulence are not yet fully understood in this context, this formulation was shown to be a more accurate method of calculating added turbulence intensity in the findings ~~of Chamorro and Porté-Agel (2011). This study states~~ Chamorro and Porté-Agel (2011), which found that turbulence intensity typically accumulates over two to three turbine rows, but then levels off to an equilibrium at this point. ~~In~~

Based on the original definition proposed in Crespo and Hernández (1996), the following expression ~~is presented to~~ in

175 Eqn. 10 has been tuned through comparisons to high fidelity CFD simulations (King et al., 2020) and several field studies (Fleming et al., 2019, 2020b) to accurately calculate the added turbulence due to upstream turbine j:

$$I_j^+ = A_{\text{overlap}} \left(\underline{0.8}0.5 a_j^{\underline{0.73}0.8} I_0^{\underline{0.35}0.1} (x/D_j)^{-0.32} \right), \tag{10}$$

where D_j denotes the diameter of turbine j, and A_{overlap} refers to the fraction of the rotor-swept area of the downstream turbine that intersects with the cross-sectional area of the wake from the upstream turbine. The axial induction factor, a_j is evaluated

180 based on the value of C_T, as defined in Burton et al. (2002) and Bastankhah and Porté-Agel (2016).

As noted earlier, the Gaussian wake model was developed under the assumption of flat terrain. Since the heterogeneous model was specifically designed to best benefit wind farms located in complex terrain, it important to know the consequences of violating this assumption. In Fleming et al. (2020b), a field study is presented that focuses on analyzing the performance of the tuned parameters in Eqn. 10, by comparing two campaigns located in comparatively simple and complex terrains.

185 The findings of this study indicate that inaccurate tuning of the tuned variables may worsen FLORIS's typical tendency to underpredict wake losses in areas with complex terrain.

3 Changes to the FLORIS model

Previously, FLORIS derived the initial wind speed, wind direction, and turbulence intensity by using one value to represent the entire flow-field domain. In this article, we describe the modifications to FLORIS to accommodate heterogeneous flows.

190 This section will explain the methods used to calculate wakes based on the gradient of values ~~in the flow field~~observed in the undisturbed flow field without wake effects. The motivation behind this development was to create a more detailed characterization of the initial state of the atmosphere, which leads to improvements in the power predictions of a wind farm.

3.1 Initializing the heterogeneous flow field

To implement heterogeneity in FLORIS, an interpolation is performed based on several input values assigned to spatially

195 varying coordinates inside or adjacent to the wind farm ~~.~~ (see Fig. 2a). These initial inputs are used to approximate the value of atmospheric characteristics at the location of every turbine within the wind farm, and at each individual grid point of the FLORIS flow field. FLORIS performs methods of interpolation and extrapolation using software packages provided by SciPy: an open-source scientific computing library for the Python programming language (Virtanen et al., 2020). The packages used in this method include a piecewise linear interpolant and a nearest neighbour interpolant, which are combined to create an

algorithm that calculates a unique value for each x and y coordinate within the flow field. Fig. 1 shows a pseudo-code diagram of this process for reference.
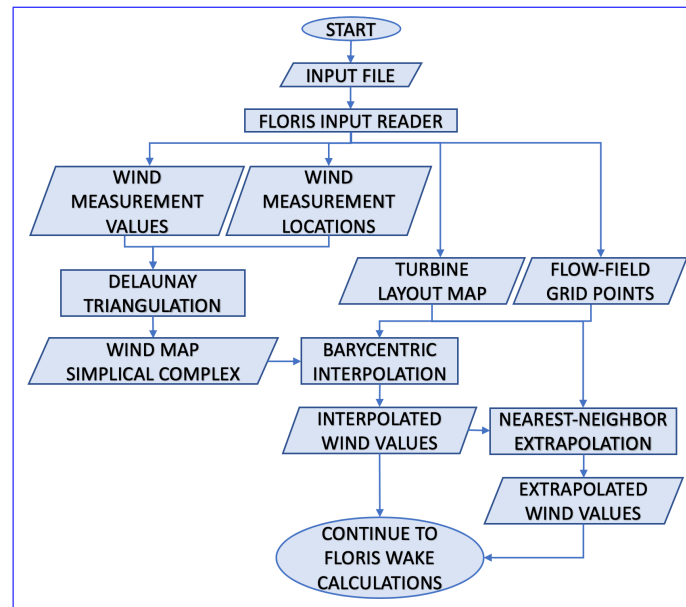
Figure 1. A diagram representing the processes performed during the initialization of the heterogeneous FLORIS model.

The process begins with implementing a piecewise linear interpolation method for all points within the region defined by the input coordinates. First, Delaunay triangulation is performed using the Quickhull algorithm discussed in Barber et al. (1996). This method forms triangular connections between input points, based on their relative coordinates, and defines each triangle by ensuring its circumcircle remains empty. The result of this triangulation generates a mesh of triangular elements called a simplicial complex. Further details on the concept of Delaunay triangulation are explained in-depth in Shewchuk (1999) and Barber et al. (1996).

The next step in determining the interpolated values is to use the established triangular elements to perform barycentric interpolation. During this step, the barycentric coordinates of each point of interest are determined relative to the triangular element in which it resides. Based on each set of barycentric coordinates, the interpolated result is calculated using a weighted average of the values defined at the triangle's vertices (Floater, 2015). A visual depiction of the methods utilized in this piecewise interpolation method (Delaunay Triangulation and Barycentric Interpolation) are shown in Fig. 2ab. After these processes are complete, FLORIS assigns the interpolated values to each flow-field grid point and turbine location inside the triangulated region bounded by the input coordinates. Any points that fall outside of this region must be determined through additional extrapolation processes.

(a) Initial inputs and turbine locations.

(b) Delaunay triangulation and Barycentric interpolation.
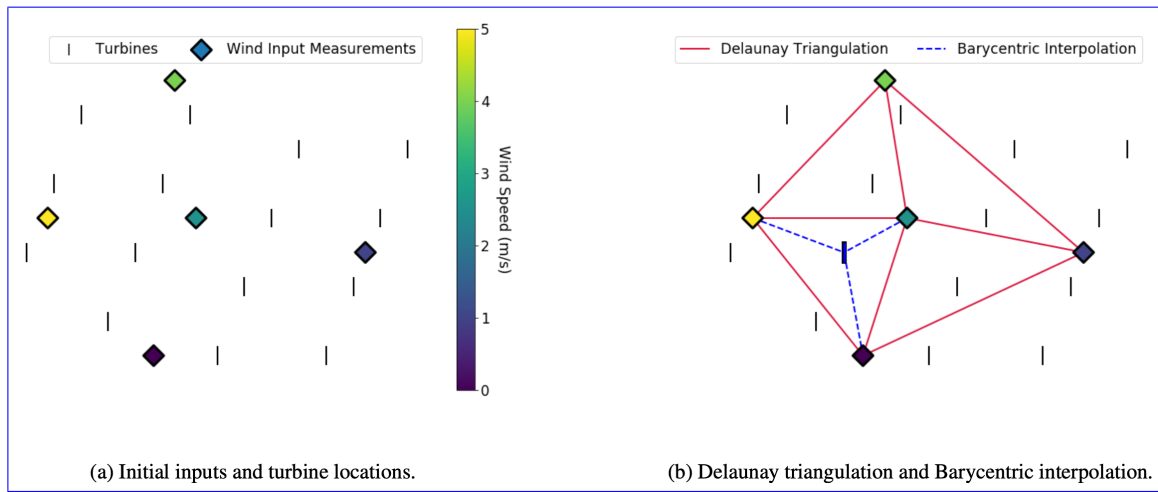
Figure 2. A visual depiction of the methods used interpolate and define atmospheric characterization values at specific points within the input coordinates.

Linear Barycentric interpolation was chosen to implement for this step because it is relatively efficient in computation and can be easily implemented without requiring any input parameters other than the locations and values of wind measurements. Although it must be noted that the accuracy of the interpolated values is dependent on the quality of input measurements provided, the complexity of the terrain geometry, and the weather patterns observed in the physical wind farm.

220   The extrapolation process implements a nearest-neighbor interpolant to calculate all remaining unknown values. Using the recently interpolated point values in addition to the original input values, this method operates by selecting a single value at the nearest location to the point being extrapolated, and assigning this nearest value to the extrapolated point. A visualization of this calculation is depicted in Fig. 3.

(c) Nearest-neighbor extrapolation.

(d) Final result of the interpolation and extrapolation processes.
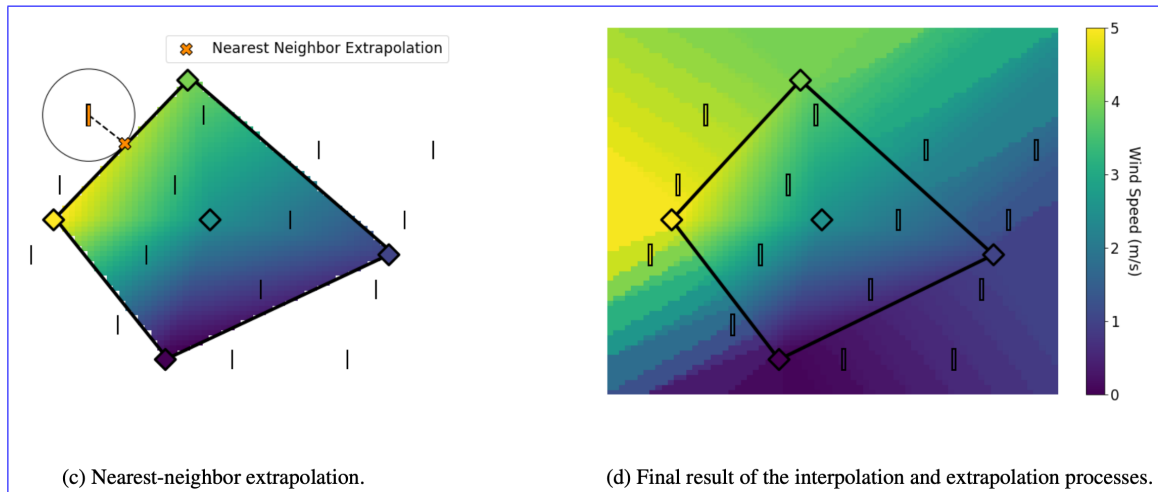
Figure 3. The extrapolation process used to define the remaining values for characterization of the initial state of fluid flow.

9

~~This combination of interpolation and extrapolation methods~~ The nearest-neighbor extrapolation method was chosen because it defines a feasible relationship between input measurements and does not attempt to extrapolate using a formula derived from a curve-fitting or trend-predictive algorithm. Many other extrapolation methods attempt to predict a rate of change outward of the interpolation domain by implementing a function that approximates a predicted progression of extrapolated values. ~~It~~ For example, it was found that the ~~extrapolation performed by these algorithms often produced results that were outside the range of possible values for~~ analytic continuation of Radial Basis Functions (RBF) and fitted polynomial splines outside of the initial domain often produced a non-feasible output that did not respect the physical limitations of the atmospheric characteristic being ~~defined. Because of this issue of infeasible outputs, these methods were consequently avoided for this purpose.~~ extrapolated. Although it was speculated that these methods could likely be adjusted with tuning factors to fit extrapolated data within feasible bounds, efforts to do this were not explored in this study. Instead, the nearest-neighbor algorithm was chosen to simplify implementation of realistic extrapolation within the model.

When solving for the interpolated and extrapolated values for turbulence intensity and wind speed, values are easily computed because they are defined by values on a ~~noncyclical~~ non-cyclical scale. Because wind direction is represented using angles in degrees, the interpolation and extrapolation methods must be circular. The issue of interpolating circular data was addressed by simply computing the interpolation twice for each angle of wind direction, Φ: once for the cosine component, α, and again for the sine component, β. The wind direction in a wind farm, Φ, can be defined as:

$$\Phi = \arctan 2 \left(\frac{\beta}{\alpha} \right) \tag{11}$$

Where ~~$\alpha = cos\ \Phi$, and $\beta = sin\ \Phi$~~ $\alpha = \cos \Phi$, and $\beta = \sin \Phi$. After Φ is computed, the wind direction interpolation can then be defined for the entire wind farm.

It should be noted that the vertical (z) dimension is not considered when interpolating and extrapolating from the atmospheric inputs. Instead, all input values are assumed to be at the same z location, and the interpolation is performed on a two-dimensional plane at this height. Although this approximation may result in a less accurate result, this approach allows the interpolation and extrapolation algorithm to operate with less computational cost.

3.2 Heterogeneous wind speed

Before FLORIS performs any calculations for velocity deficit in wakes, it first assigns an initial value of wind speed (U) to each grid point in the flow-field grid. In a homogeneous case, these grid points would all have the same value across an $x - y$ plane, but in a heterogeneous case, these grid points all have different values, dependent on the initial values that have already been established through interpolation. After U is defined at each grid point, the wind-speed values at each x, y, and z coordinate in the flow-field domain are defined as U_{init}, calculated using the power law in Eq. 7. From this point, the calculation of wakes proceeds in the same way as the homogeneous cases, with the exception of a more complex algorithm for accounting for changes in wind direction, as explained in Section 3.3. The velocity deficit behind each turbine is calculated by applying

255 Eq. 4 from Section 2.3.1, where the free-stream velocity (U_∞) in Eq. 4 is defined as the local U_{init} values at each flow-field grid point. Figure 4 shows visualizations of the resulting wakes after subtracting the calculated velocity deficit from the initial free-stream velocity at each flow-field grid point.
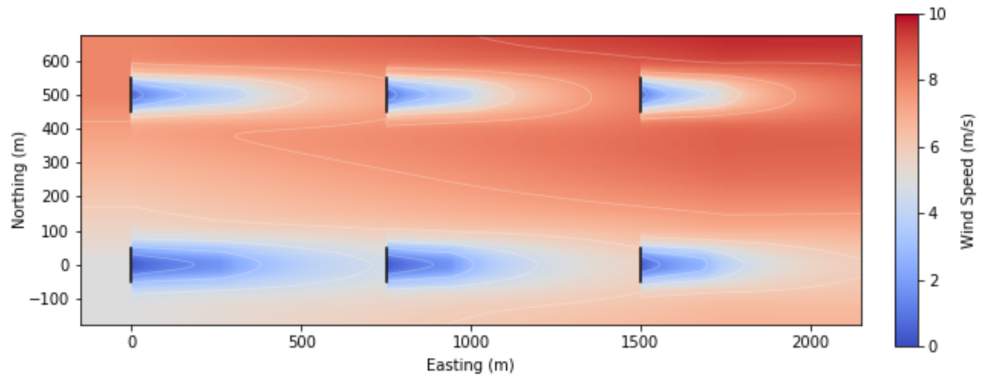
(a) Horizontal plane of the FLORIS simulation, taken at the turbine hub height (90m).
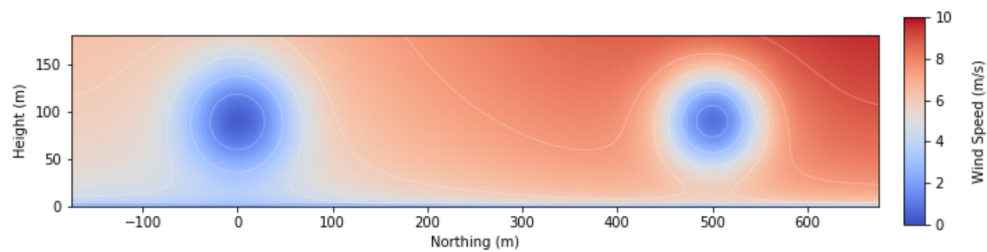
(b) Vertical cross-plane of the FLORIS simulation, taken at 760m east of the origin (10m downstream of middle turbines).

Figure 4. Visualizations of two planes showing the FLORIS flow field during a simulation with heterogeneous wind speed.

3.3 Heterogeneous wind direction

Similar to wind speed, an interpolation of wind direction is initially established across the flow-field grid through the methods
260 of interpolation discussed in Section 3.1. The input values of wind direction are defined so that 270 degrees represents wind movement from west to east (see Fig. 5a), then once FLORIS begins computations with these wind directions, the values are converted so that 0 degrees represents the wind traveling from west to east (see Fig. 5b). Using these wind direction values, the turbine coordinates are rotated about the center of the flow field at these angles, as exemplified in Fig. 5b.

(a) Interpolated values of wind direction, defined at every point within the flow-field domain.

(b) Rotation of turbine locations relative to the center of rotation.
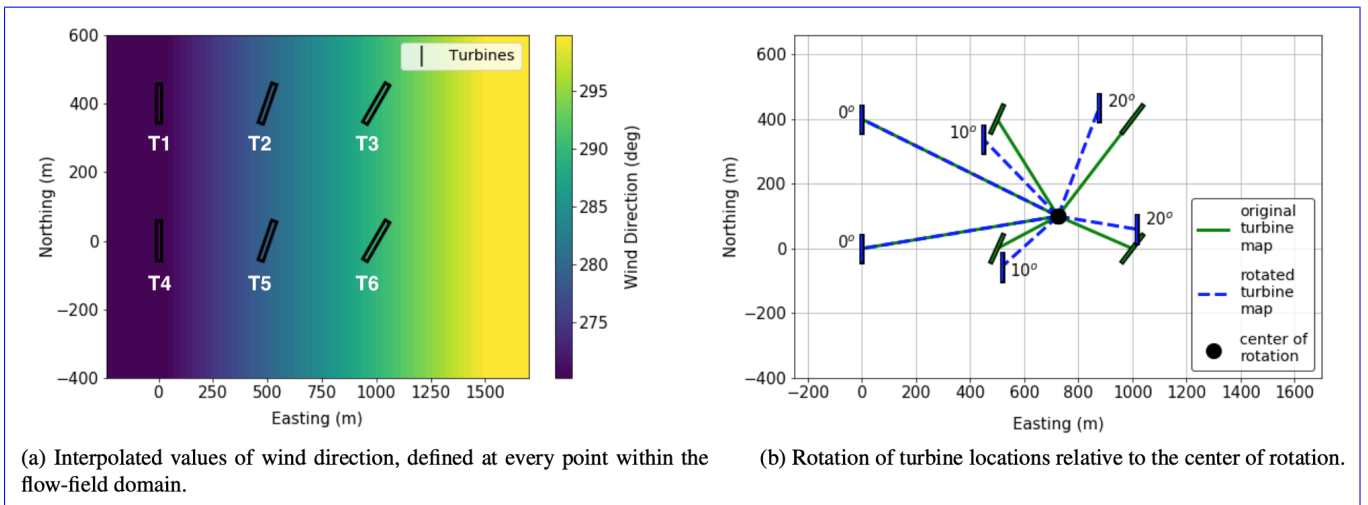
Figure 5. A depiction of the initial processes before the calculation of wakes. Figure 5a shows the result of wind direction interpolation, and Fig. 5b shows the process used to define the location of the rotated turbine map. The turbines will be referred to individually as T1, T2, ... T6, as defined in Fig. 5a.

Using the rotated turbine map shown in Fig. 5b for reference, the flow field is adjusted to calculate each turbine wake independently, starting with the turbine that is the furthest upstream. To initiate the rotation of the flow-field grid, the grid points are rotated to the angle that is defined at the given turbine. This initial step is exemplified in Fig. 6 for the calculation of the velocity deficit behind turbine T6 only, but this will also be repeated for each turbine in the entire wind farm. This step is necessary to put the original non-rotated grid points in a frame of reference relative to the each specific turbine as their particular wake is calculated.

(a) Non-rotated (original) flow-field grid points, showing all but one of the turbine wakes calculated.

(b) The flow-field grid points are rotated about the center of rotation using the wind direction defined at the lower right turbine (20°), and translated to be aligned with the location of the turbine.
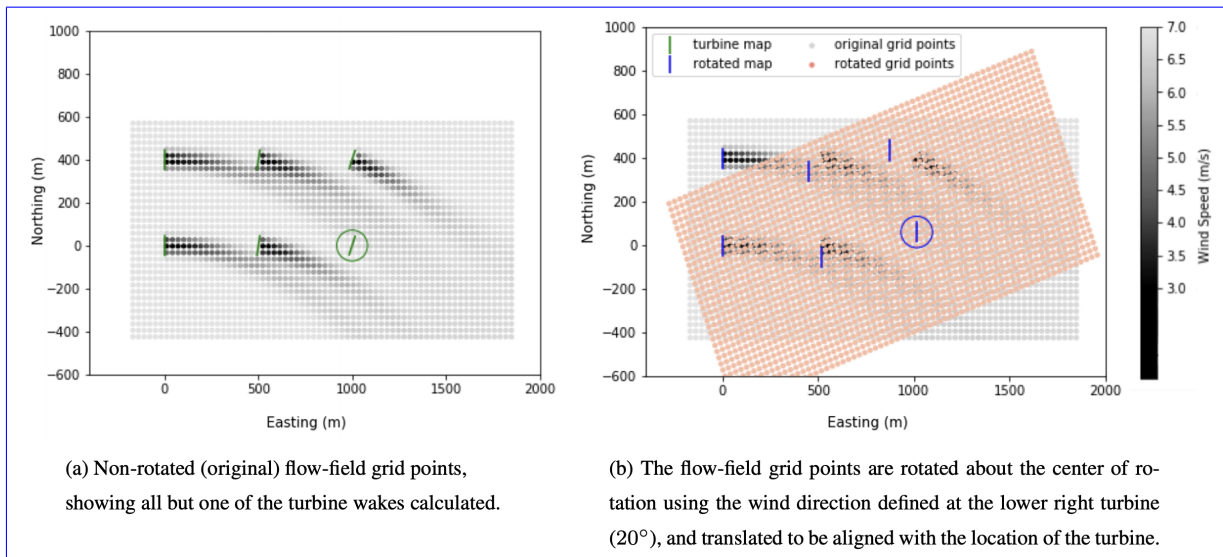
Figure 6. Depiction of the process performed in FLORIS to align the flow-field grid with the location and wind direction of ~~a given~~ turbine T6 (as defined in Fig. 5a).

270   Next, to calculate the velocity deficit caused by each turbine's wake, all of the grid points in the flow field are rotated to replicate the effects of changing wind direction. These rotated grid points represent the redirection of the flow in response to changing wind direction within the flow field (see Fig. 7a). Once the velocity deficit has been calculated using the rotated grid points, the ~~grid~~ points are rotated back to their original positions in the flow field. Fig. 7b shows the product of the final step, where the calculated velocity deficit is subtracted from the initial free-stream velocity at each flow-field grid point to reveal the

275   resulting shape of the wake.
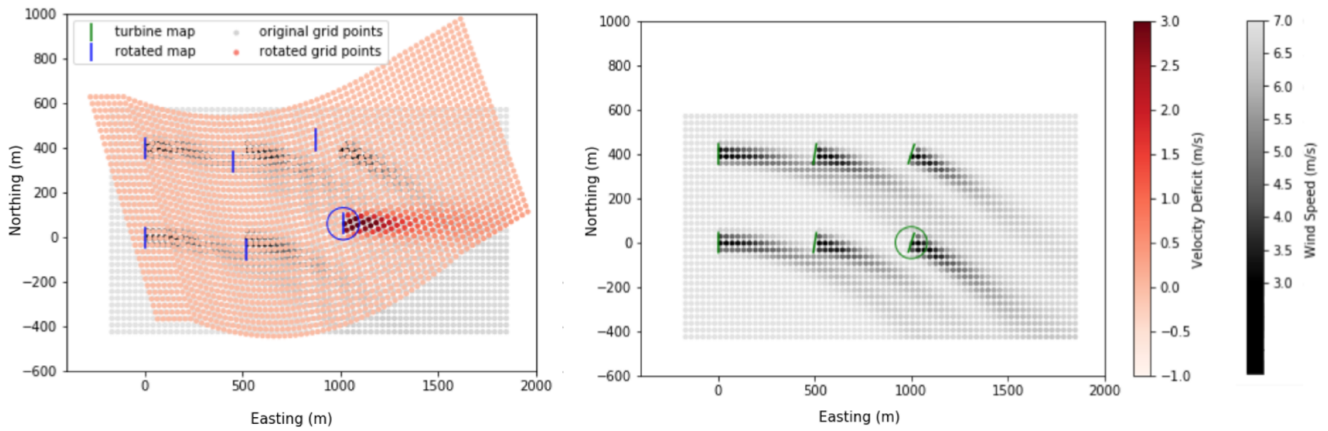
(a) Rotated grid points used in FLORIS to calculate the velocity deficit behind a turbine.

(b) Non-rotated (original) flow-field grid points showing resulting wake calculations.

Figure 7. Visualizations of FLORIS calculating velocity deficit ~~behind a~~ turbine T6 in conditions of heterogeneous wind direction. The velocity deficit is calculated using the grid points in the fully rotated position (Fig. 7a), and then applied to the free-stream velocity defined at the grid points in their original non-rotated location (Fig. 7b).

As discussed in Section 2.2, there is a minor computational expense in simulating the flow field independently for each turbine in the wind farm. This is because FLORIS determines a unique set of rotated grid points relative to the wind direction and coordinates of each turbine separately. The grid spacing in the streamwise (x) direction relative to the direction of flow is kept uniform throughout each iteration of the rotated grid, but the spanwise (y) spacing is adjusted with respect to the local

280   wind direction inside the flow field. This allows the model to replicate a gradual change in wind direction throughout the flow field. The resulting flow-field wake calculation is shown in Fig. 8.
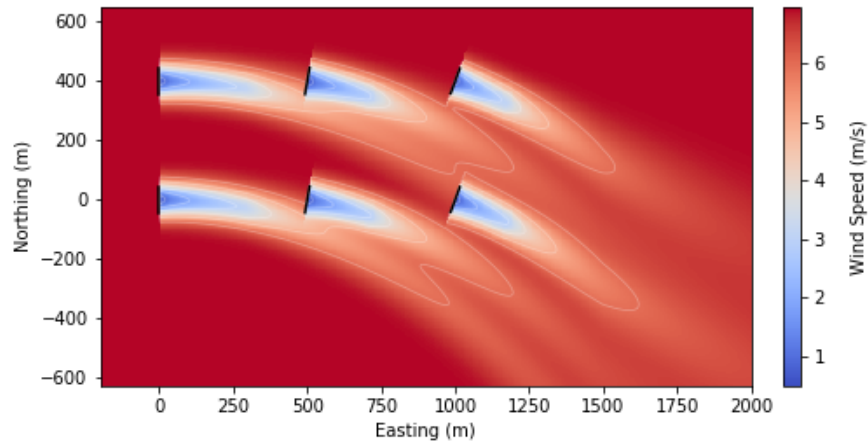
Figure 8. Visualization of a flow field with heterogeneous wind direction. Turbine rotors are indicated by black lines.

The grid point spacing in the x direction must be kept constant to avoid elongation or distortion of wake propagation and placement. Because the grid spacing in the y direction is not kept uniform, it must be noted that this capability of emulating a gradual change in wind direction may prevent the model from conserving momentum in some situations. Methods of enforcing uniform spacing in the y direction for each individual turbine wake have been developed, but are not currently implemented because doing so limits the model's ability to create a gradient of wind directions within the flow field. In future work, methods of enforcing momentum conservation in this algorithm will be further investigated.

To further exemplify the applications of this functionality, Fig. 9 shows a more complex simulation of non-constant heterogeneous wind direction simulation in an irregularly spaced wind farm. The steps that FLORIS performs to evaluate this flow condition are identical to the ones displayed in Figs. 5 - 7, except it is personalized to the more complex variations of the depicted state of flow.
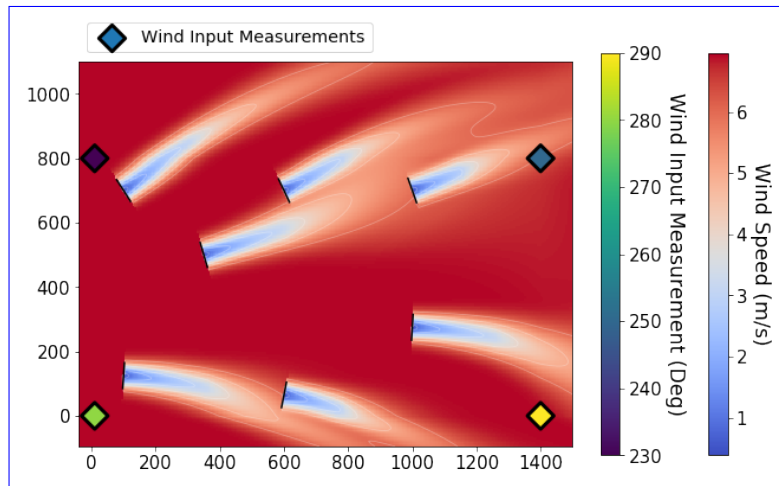
Figure 9. A second visualization of a flow field with more complex heterogeneous wind direction. Wind input measurements are indicated using diamond markers, and turbine rotors are shown with black lines.

It is important to consider that this model was not designed to calculate the effects of changes in wind direction that are ~~greater than 90 degrees. Though these flow conditions may not be typical of most wind farms, a~~ extremely dynamic. The limiting case of wind direction change is that which causes the flow-field grid points to conflict in the rotated grid produced during the velocity deficit calculations shown in Fig. 7 and 6). This limit also must be determined for each farm independently, depending on the site-specific layout geometry of each case. A change in wind direction that is too drastic ~~results in~~ causes an overlapping of portions of the rotated flow-field grid points~~. This effect causes an~~, which results in erroneous assignment of velocity deficit to the overlapped points ~~of~~ in the flow-field grid.

Although it may be possible for the wind direction within a wind farm to change this drastically, these conditions often involve multiple adjacent domains of flow that are separated by a boundary, which are difficult to represent in this model. These weather conditions are also most often observed in instances of lower wind speeds, and therefore can be considered

not as lucrative in regards to power production. Plans for future developments to FLORIS involve designing a more inclusive model that is capable of mitigating issues with large shifts in wind direction.

3.4 Heterogeneous turbulence intensity

305 The geographic distribution of turbulence intensity is established for the initial state of the flow field through the interpolation methods discussed in section 3.1. This strategy of defining a more detailed variation of turbulence intensity in the flow field makes approximation of wake dissipation and deflection more accurate, therefore improving the estimation of the effect of nearby turbine operation within a wind farm. The implementation of heterogeneous turbulence intensity and heterogeneous wind speed are similar, in that the initial heterogeneous conditions are established throughout the flow field by interpolating

310 from the input values, and then waked conditions are updated throughout FLORIS computations of flow-field interactions. During the calculation of wakes, the ambient turbulence intensity that is initially defined at each turbine location is continuously recalculated to account for added turbulence intensity resulting from turbine wakes up to $15D$ upstream, as previously discussed in Section 2.3.2 and in Niayifar and Porté-Agel (2015). ~~In~~ A horizontal plane of a FLORIS simulation featuring heterogeneous turbulence intensity can be observed in Fig. 10.
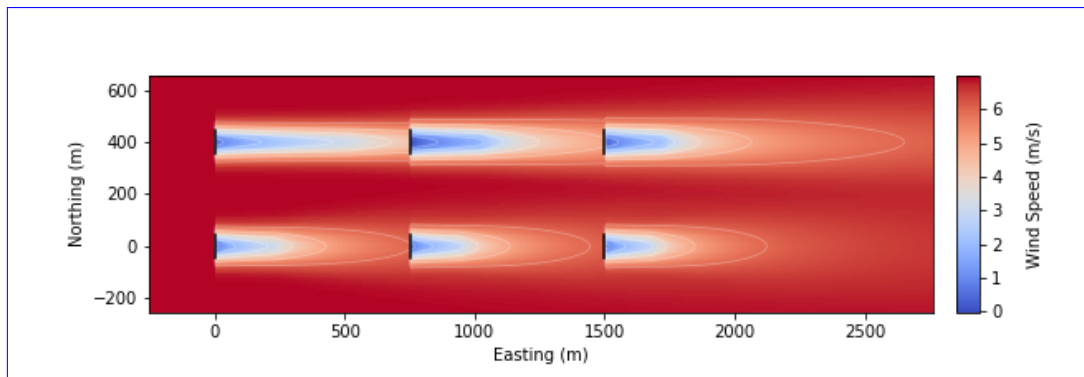
Figure 10. Visualization of a flow field with heterogeneous turbulence intensity. The turbines that experience higher turbulence intensity show a faster rate of wake recovery, and vice versa. Turbine rotors are indicated by black lines.

315 It is important to note that in the interest of conserving computational efficiency, calculations for evaluating the rate of wake expansion and recovery are only dependent on the updated turbulence intensity at the location of the turbine creating the wake. ~~A horizontal plane of a FLORIS simulation featuring heterogeneous turbulence intensity can be observed in Fig. 10.~~

~~Visualization of a flow field with heterogeneous turbulence intensity. The turbines that experience higher turbulence intensity show a faster rate of wake recovery, and vice versa. Turbine rotors are indicated by black lines.~~

320 3.5 Turbulence correction

In addition to the heterogeneous features, developments were also made to reduce inaccuracies in power-output predictions caused by turbulent operating conditions. As mentioned in Section 2.1, the accuracy of the zero-turbulence power curve is

compromised in conditions of varying turbulence intensity. The revised power calculation, presented in this section, includes a parameter that approximates the effect of turbulence intensity on the power output of a turbine in a wind farm.

325   Specifically, this approach adjusts the power output with respect to the level of turbulence intensity at a turbine. The adjusted power is calculated by using distribution of the wind-speed fluctuations at the turbine, based on calculations that consider the original wind speed and the standard deviation in wind speed. The first step in this algorithm is to create a normalized probability density function, $f(x)$, of wind speeds, x, evenly distributed within the domain of one standard deviation from the mean wind speed, μ. The standard deviation, σ, is determined by multiplying the turbulence intensity at the turbine by the

330   mean wind speed, μ. Wind speeds that are greater than the cutout wind speed are omitted.

    The value of the power coefficient, C_P, in the power table is also determined at each wind speed, x_i, and at the original wind speed (μ). The ratio of the adjusted power (P_{adj}) to the original value of power (P_0) is referred to as the turbulence parameter, Λ. The turbulence parameter can be calculated by summing the weighted adjusted values of power in the following expression, for each wind speed, x_i, in the domain of the probability density function, $f(x_i)$:

335 $$\Lambda = \frac{P_{adj}}{P_0} = \frac{\int_{x_1}^{x_{100}} f(x_i,\mu,\sigma)C_{P,i}x_i^3\, dx}{C_{P,\mu}\mu^3} \frac{\int_{x_1}^{x_{100}} f(x_i,\mu,\sigma)C_{P,i}x_i^3\, dx_i}{C_{P,\mu}\mu^3} = \frac{\sum_{i=1}^{100} f(x_i,\mu,\sigma)C_{P,i}x_i^3}{C_{P,\mu}\mu^3},$$ (12)

where the integral of $f(x_i)$ is approximated by taking 100 samples of the $f(x_i)$. The resulting power curves depending on turbulence intensity are shown in Fig. 11. As the turbulence intensity increases, the power output increases in Region 2 and decreases across Region 3.
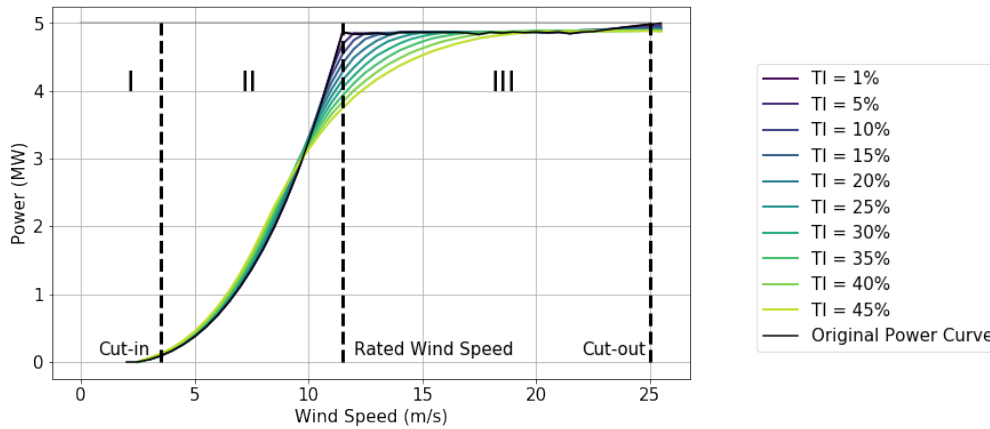
Figure 11. Adjusted power curve for the NREL 5-MW reference turbine for different turbulence intensities. The dashed lines denote the cut-in, rated, and cut-out wind speeds, and also represent the boundaries of the first, second, and third regions, respectively.

The following expression may be used to calculate the final value of adjusted power output, P_{adj}, with respect to the current turbulence intensity at a turbine:

$$P_{adj} = P_0 \Lambda = \frac{1}{2} \rho A C_{P,\mu} \underline{cos} \cos(\gamma)^p \mu^3 \Lambda. \tag{13}$$

Where γ is the yaw angle of the turbine, and Λ represents the turbulence parameter. The value of Λ must always be greater than zero.

~~Although it was not explored for the purpose of this article~~In future work, this turbulence-correction model could be improved by implementing a similar consideration of the thrust coefficient, C_T. Because ~~rotor thrust is calculated from an equation that is also dependent on wind speed,~~ the velocity deficit computations in this model rely on the value of C_T, it may be advantageous to expand this method to calculate an adjustment parameter for the effects of turbulence on rotor thrust.

It is important to note that similar models have been developed that incorporate methods of turbulence re-normalization based on machine-learned or empirically-derived data (Clifton and Wagner, 2014). The proposed method discussed in this section was developed to attempt to represent the variation of power output due to turbulence effects, while using a simple strategy that is not dependent on the availability of data other than the current wind farm atmospheric measurements, and the power curve provided by the turbine manufacturer. In future work, it may be ~~possible to create a similar correction model to improve FLORIS estimates in the future~~advantageous to incorporate more complex techniques that are able to capture the effects of turbulence intensity with greater detail and accuracy.

4 Results

A series of simulations were performed to analyze the effectiveness of the changes implemented in FLORIS. A large, utility-scale wind farm located within ~~complex~~ mountainous terrain was chosen for this study because it is often subject to unpredictable and dramatic shifts in weather conditions. More information regarding the physical layout and characteristics of this wind farm can be found in Appendix A. The motivation behind performing these simulations was to quantify the effect of the recent developments to FLORIS in reducing the error in power-output predictions for wind farms in complex terrain.

FLORIS simulations were performed using heterogeneous inputs of wind direction, turbulence intensity, and wind speed, which were taken from the wind farm's SCADA records. These inputs include ~~five~~ four wind measurement values for each atmospheric characteristic, derived from Meteorological (MET) tower measurements placed in various locations throughout the wind farm. Similar simulations were performed using an identical FLORIS model, but with a singular homogeneous input for wind speed, wind direction, and turbulence intensity. These homogeneous inputs were derived by evaluating the average of the five heterogeneous input values at each time step. The resulting power output of all simulations was recorded with the inclusion of the turbulence correction and without. All cases were simulated using data averaged at time steps of ~~30~~ 10 minutes over a range of 2 months.

4.1 Performance results

370 This section presents the results from all FLORIS simulations and analyzes the accuracy of power predictions from each test case with respect to the actual-to-power output of the wind farm recorded from the SCADA system. Fig. 12 includes two horizontal planes showing a partial section of heterogeneous flow calculations during these simulations. This figure demonstrates the visual capabilities of the heterogeneous model and how the effects of the new wake calculations can be translated into visual information for further analysis of wake interactions within a wind farm.
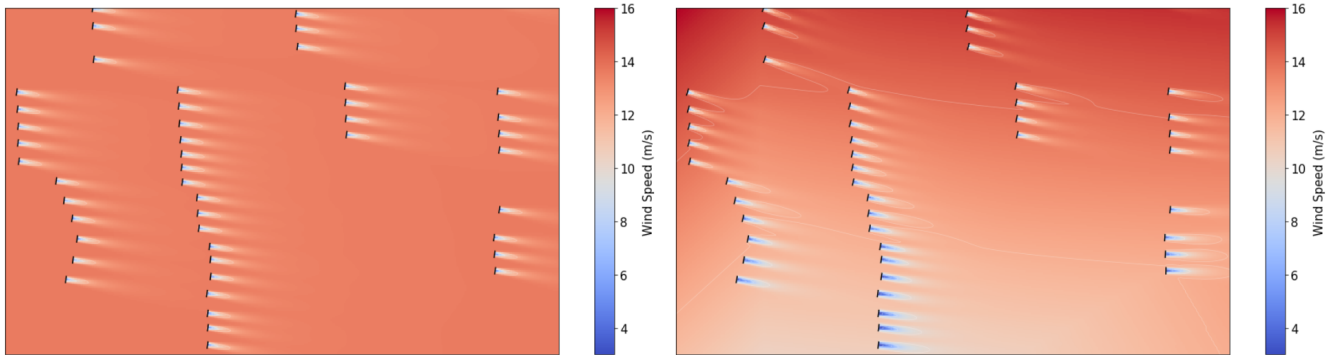
(a) Horizontal plane of a FLORIS simulation using the homogeneous model. (b) Horizontal plane of a FLORIS simulation using the heterogeneous model.

Figure 12. Horizontal planes of two different FLORIS simulations, taken at the same time-step iteration.

375 Although these visualizations do not give direct estimates of power prediction, they are helpful in translating the input measurements into a form that characterizes the general behavior of wind farm dynamics for the interpretation of the observer. The cut plane visualization is helpful in performing qualitative analysis of turbine wake interactions, and is more useful when displaying the estimated weather conditions characteristic of each location in the flow field, as shown in the heterogeneous model.

380 When comparing the performance of the simulations, the calculated power output was tabulated and compared, for accuracy. In Fig. 13~~and Fig. ??~~, the sum of wind farm power output from each FLORIS simulation is normalized ~~and plotted~~ with respect to the rated power output for the wind farm, and plotted along with the recorded SCADA output. This approach highlights any weaknesses in each model relative to the overall performance of the others. ~~Two different~~ A 24-hour ~~periods were~~ period was chosen to demonstrate how the models performed under ~~different~~ average diurnal conditions. Figure 13 shows a day with

385 relatively variant weather conditions and many ~~large~~ rapid shifts in power output~~, whereas Fig. ?? shows the performance of the models on a day showing a more gradual shift in weather conditions. These days are referred to as Day A and Day B, respectively.~~.
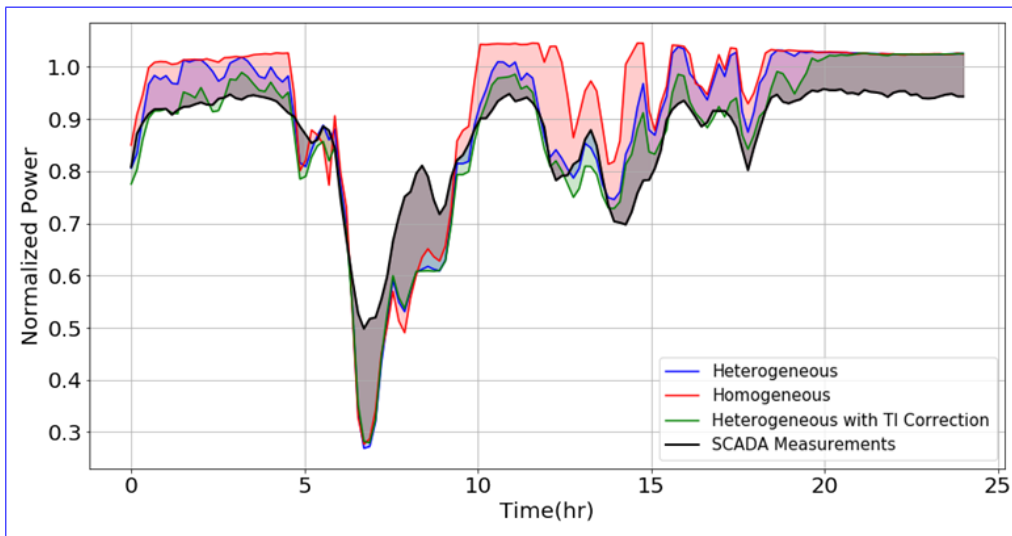
Figure 13. ~~Day A: Large atmospheric variations throughout the day.~~ Power output calculated by FLORIS for homogeneous (red), hetero-geneous without the turbulence correction (blue), and heterogeneous with the turbulence correction (green), compared with SCADA data shown in black. Each shaded region represents the difference between predictions of power output, and the measured power output from SCADA data.

~~Day B: Smaller atmospheric variations throughout the day. Power output calculated by FLORIS for homogeneous (red), heterogeneous without the turbulence correction (blue), and heterogeneous with the turbulence correction (green), compared~~
390 ~~with SCADA data shown in black. Each shaded region represents the difference between predictions of power output, and the measured power output from SCADA data.~~

It is evident from the ~~plots of Figures 13and ??~~ plot in Figure 13, that the heterogeneous models are predicting the power output ~~during these 2 days~~ more accurately than the homogeneous model. The trend line of the heterogeneous simulations consistently follows closer to the line representing the power output recorded from SCADA data. Additionally, the heteroge-
395 neous simulation that included turbulence-intensity corrections showed an extra advantage in estimating turbine performance, following closely to the trend line of the heterogeneous simulation, and also reliably contributing error-reducing improvements to the heterogeneous model. While this juxtaposition is effective in ranking each model's ability to estimate total farm power output, it should be noted this comparison only indicates the accuracy of a ~~calculation~~ calculations for the entire wind farm power output ~~as a sum of its individual turbines~~ collectively without considering the accuracy at each turbine individually.

400 It is possible for wake models to overpredict the power output of some turbines, and underpredict others, in a way that produces a total wind farm power estimate that seems accurate, but is not using reliable and precise methods of calculation. To verify that the recent additions to FLORIS have improved the power-predicting capabilities, it must be confirmed that the new model produces a consistently accurate estimate with respect to each iteration in the time series and each turbine within the wind farm individually. To prove this model's consistency in accuracy, the normalized absolute error was calculated at each
405 turbine at each iteration of the time series for ~~days A and B. The the~~ this same day. The sum of the absolute error at all turbines

20

within the wind farm is calculated for each simulation model at each time iteration. To calculate the sum of absolute error (SAE) for all turbines, the following formula was applied to each time iteration of the simulation.

$$SAE = \sum_{i=1}^{n} |P_{model,i} - P_{actual,i}|, \tag{14}$$

where n is the number of turbines in the wind farm, $P_{actual,i}$ is the measured power output of turbine i, and $P_{model,i}$ is the predicted power output of turbine i from a given FLORIS model. The results of each FLORIS model were calculated and plotted on the same set of axes in ~~Figures 14and ??~~Figure 14.
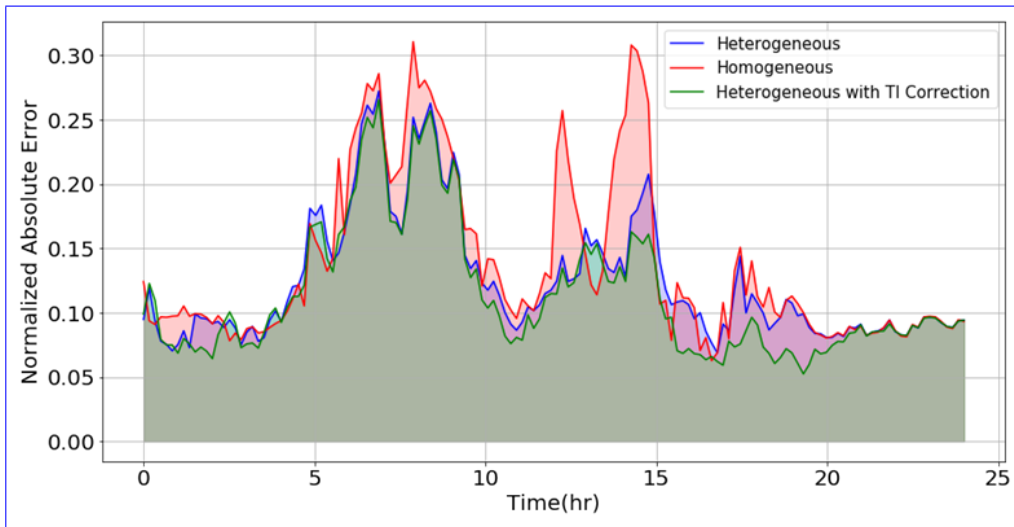
Figure 14. Day A: Sum of the normalized absolute error at each turbine in the wind farm, computed at each time step.

~~Day B: Sum of the normalized absolute error at each turbine in the wind farm, computed at each time step.~~

The trends observed in ~~Figures 14 and ??~~ Figure 14 exhibit similar characteristics that indicate the accuracy of the model at each turbine is increasing with the application of the heterogeneous model and turbulence-intensity correction parameter. The heterogeneous model reliably produces less error when calculating the power at each turbine over the time series, which ensures that the power predictions of the entire farm are not self-compensating because of simultaneous overpredictions and underpredictions of individual turbine outputs. Furthermore, if ~~the plots of Figures 14 and ?? are~~ Figure 14 is analyzed with respect ~~to their corresponding~~ the trends of normalized power in ~~Figures 13and ??~~Figure 13, it is evident that the ~~additions~~ addition of heterogeneity and turbulence-intensity corrections contribute improvements to the accuracy of FLORIS power predictions in instances of overprediction and underprediction, and transitions between the two with relative consistency.

To ensure these same trends of accuracy persist over the entire two-month period, the percent error of the total wind farm power output was calculated at each time-step iteration using the following equation.

$$Percent\ Error = \frac{|P_{model} - P_{actual}|}{|P_{actual}|}, \tag{15}$$

where P_{actual} is the measured power output of the wind farm, and P_{model} is the power output of the wind farm predicted by a given FLORIS model. The results of these calculations were grouped into three separate domains: wind speeds of less than 5 m/s, wind speeds in the range of 5 to 11 m/s, and wind speeds greater than 11 m/s. Time iterations when wind speed was less than the cut-in wind speed (2.5 m/s) were considered negligent in regards to power production and therefore omitted from the data set. A histogram of the percent error in each wind-speed domain was computed over the entire time series to display the distribution of error with respect to each simulation (Fig. 15).

(a) Percent error at all wind speeds.

(b) Percent error where wind speeds are less than 5 m/s.

(c) Percent error where wind speeds are between 5 m/s and 11 m/s.

(d) Percent error where wind speeds are greater than 11 m/s.
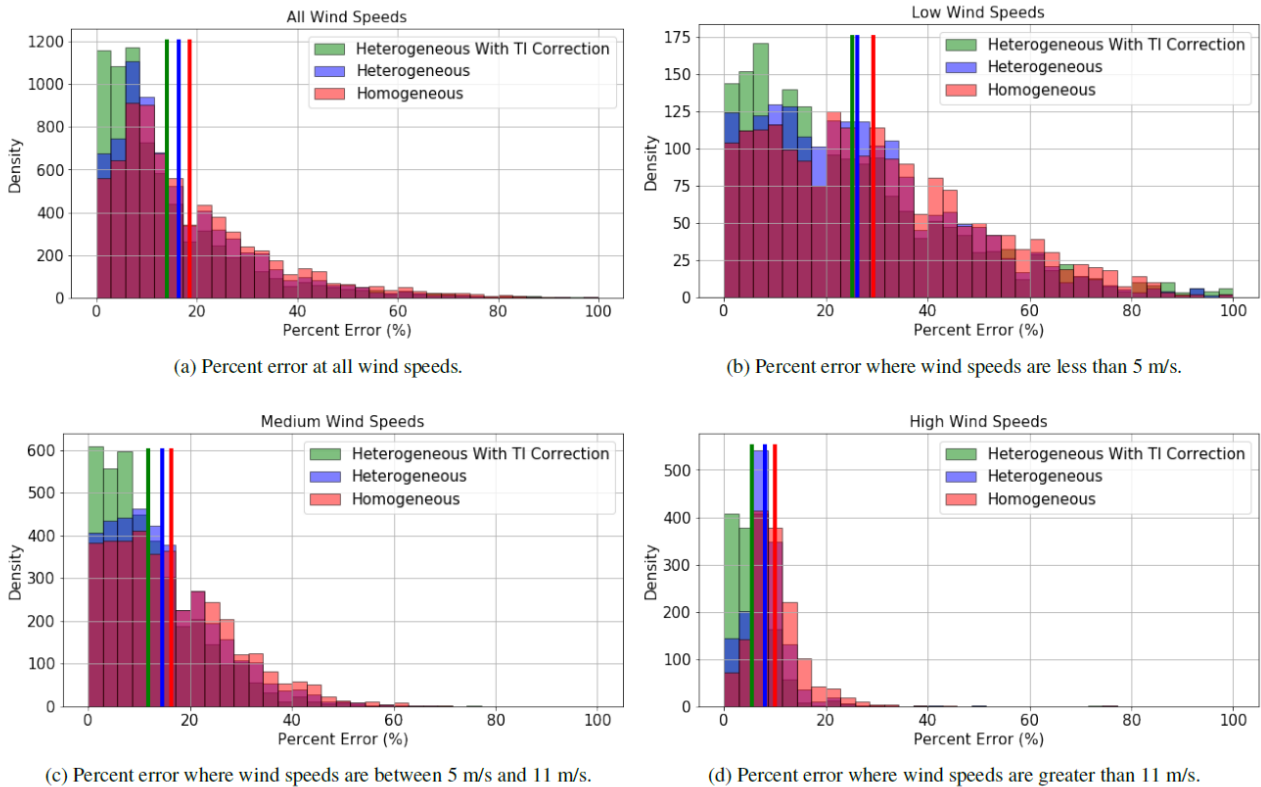
Figure 15. Percent error of all three FLORIS models, plotted for comparison within varying ranges of wind speeds.

Although the plots for the wind-speed domains vary slightly in distribution, it is clear that each histogram exemplifies a trend toward accuracy in simulations that incorporate heterogeneity and turbulence-correction calculations. It is important to

note that only the data points shown in the percent-error range of each histogram were used to calculate the respective binned averages. The outliers were omitted because they tend to skew the presentation of the data set in a way that obscures the actual trend of data.

435   The mean absolute percent error (MAPE) of all time-step iterations are also ~~tabulated~~ reported in Table 1. The data for this table was calculated by evaluating the percent error of FLORIS power predictions for the full wind farm at each time step, and then solving for the mean over the entire time series. This calculation is expressed as:

$$MAPE = \frac{1}{n} \sum_{i=1}^{n} \frac{|P_{model,i} - P_{actual,i}|}{|P_{actual,i}|}, \tag{16}$$

where n is the number of time steps in the total simulation, $P_{actual,i}$ is the recorded power output of the wind farm at time step
440   i, and $P_{model,i}$ denotes the predicted power output from the FLORIS model at time step i.

Table 1. Mean absolute percent error in total wind farm power output for all FLORIS models, tabulated for comparison within varying ranges of wind speeds.

FLORIS Simulation Model	Mean Absolute Percent Error at Wind Speed (%)			
	< 5 m/s	5 - 11 m/s	> 11 m/s	all
Homogeneous	~~41.2901~~ 43.2	~~18.0701~~ 16.3	~~9.6058~~ 10.0	~~22.8282~~ 22.4
Heterogeneous	~~46.0282~~ 48.2	~~14.5559~~ 14.5	~~7.8174~~ 8.0	~~21.9471~~ 22.5
Heterogeneous with Turbulence-~~Intensity Correction~~ Intensity Correction	~~55.4985~~ 61.4	~~10.8438~~ 11.8	~~5.0290~~ 5.5	~~22.0763~~ 24.2

When comparing the MAPE values in Table 1 with the histograms of Fig. 15, an increase in MAPE is observed in Table 1 for lower wind speeds of simulations that implemented heterogeneous and turbulence correction models. This is a trend that is not characteristic of the histograms depicted in Fig. 15b. In reference to this observation, is important to note that the metric of MAPE penalizes overpredictions with more weight than underpredictions. Furthermore, MAPE calculates mean with equal
445   weight for all time steps in the data set, which ~~allows the resulting average to be susceptible to the influence of outliers caused by instances of low power output . With these factors in mind, a~~ is often preferred for an indication of overall farm power output accuracy. It is possible that the reported increase in MAPE with lower wind speeds may be an indication that the heterogeneous and turbulence intensity correction models tend to ~~cause~~ produce more frequent overpredictions ~~in~~ of power output in conditions where wind speeds are near the cut-in speed. If this is true, further investigations may be conducted in
450   future work to determine why this is happening and how it could be circumvented.

Although MAPE is an informative metric for analyzing the average percent error relative to a specific power output range, methods that use unweighted averaging are sometimes misleading in the analysis of overall power prediction accuracy. The

relative error during time-step iterations with lower power output can seem large, even when the absolute error is insignificant in comparison to the magnitude of total farm output.

455   A more comprehensive representation of relative model accuracy is presented in the following table, where the mean absolute error (MAE) is evaluated for total wind farm output. This was calculated by evaluating the absolute error at each time step, and then taking the mean of these error values. This calculation is expressed in the following equation.

$$MAE = \frac{1}{n}\sum_{i=1}^{n}|P_{model,i} - P_{actual,i}|, \tag{17}$$

where all variables are defined similar to Eq. 16.

460   By taking an average of absolute errors instead of relative errors, MAE is a more effective metric in representing the overall accuracy of total wind farm power prediction. The resulting MAE values are shown in Table ~~??~~2, where a clear trend of increased accuracy is observe for models that implement heterogeneity and turbulence-adjustment calculations.

Table 2. Mean absolute error in total wind farm power output for all FLORIS models, tabulated for comparison within varying ranges of wind speeds. Total rated wind farm output was scaled to 100 MW for reference.

FLORIS Simulation Model	Mean Absolute Error at Wind Speed (MW)			
	< 5 m/s	5 - 11 m/s	> 11 m/s	all
Homogeneous	~~1.2605~~4.7	~~6.6785~~25.7	~~9.0980~~38.7	~~5.6567~~22.6
Heterogeneous	~~1.0372~~4.2	~~5.4143~~22.8	~~7.5353~~31.4	~~4.6219~~19.4
Heterogeneous with Turbulence-Intensity Correction	~~0.8257~~4.1	~~4.3212~~19.0	~~4.9834~~22.0	~~3.4832~~15.5

Lastly, values of MAE were also calculated to represent the accuracy of the model at each individual turbine within the wind farm. In almost all categories, Table 3 shows that simulations that used the heterogeneous model and turbulence correction outperformed the homogeneous model in the prediction of individual turbine power output. This should be expected, since overall farm output in Table 2 followed a similar trend.

Table 3. Mean absolute error in individual turbine power output for all FLORIS models, tabulated for comparison within varying ranges of wind speeds. Total rated wind farm output was scaled to 100 MW for reference.

FLORIS Simulation Model	Mean Absolute Error at Wind Speed (MW)			
	< 5 m/s	5 - 11 m/s	> 11 m/s	all
Homogeneous	0.046	0.244	0.199	0.152
Heterogeneous	0.041	0.208	0.191	0.133
Heterogeneous with Turbulence-Intensity Correction	0.041	0.202	0.179	0.129

The marked improvement of power predictions at each turbine location suggests that the implementation of the heterogeneous and turbulence correction methods are helping FLORIS model wakes and other farm-flow interactions with greater detail. To analyze the influence of wake effects in this study, identical simulations were performed with the omission of wake calculations, and the results for MAE at the overall farm and individual turbine levels are reported in Tables B1 and B2 in Appendix B.

As noted in Section 3.3, the implementation of methods utilized to simulate gradually varying wind direction ~~cause~~ causes the heterogeneous model to be less efficient in computation. To quantify this increased computational cost, each simulation was timed in this study. These time recordings showed that, on average, the simulations using the heterogeneous model took less than 10% longer to compute than those using the homogeneous model. The choice to sacrifice computational efficiency in the heterogeneous model was seen as a necessary trade-off to achieve greater detail and accuracy in simulations of more dynamic environments. Future developments to FLORIS will attempt to optimize the efficiency of this model, and reduce the time necessary to simulate the effects of changing wind direction.

5 Conclusions

This article introduces a method to include heterogeneous flow fields into the FLORIS simulation tool, as well as a turbulence correction to the power reported at each turbine. To analyze the developed model's improvements in accuracy, several FLORIS simulations with and without these changes were compared to SCADA data from a utility-scale wind farm. The results of the FLORIS simulations indicate that these two modifications improve power predictions of the wind farm at the turbine and wind farm level. The increased accuracy of this model's power-prediction capabilities ~~show~~ shows that this method is more precise in predicting farm-flow interaction in heterogeneous and turbulent environments, which previous versions of FLORIS were not able to simulate.

Overall, the heterogeneous and turbulence-intensity correction modifications presented in this article showed a positive effect on the accuracy of FLORIS capabilities. This improved model provides a more detailed quantitative and qualitative analysis of wind farm flow, including the demonstration of heterogeneous flow in cut-plane velocity plots, and improved accuracy in

power prediction at individual turbines as well as total wind farm power output. The FLORIS simulations that implemented the heterogeneous flow model showed a 14.6% decrease in Mean Absolute Error (MAE) of wind farm power output prediction, in comparison to the original homogeneous model simulations. With the use of the proposed Turbulence Intensity Correction method in addition to the heterogeneous model, the MAE in farm power output predictions showed a 31.42% MAE decrease compared to the homogeneous model.

These modifications to FLORIS have outlined a framework for a wake model that features atmospheric heterogeneity and turbulence-intensity corrections to the power curve and provides a platform for further developments in this area of research. ~~Although wind farm controls applications have not been tested using this algorithm,~~ In agreement with this study, the findings of Fleming et al. (2020a) also ndicate that this model shows promise in enhancing the performance of FLORIS's existing wind farm optimization controls~~. In future work, a study of~~, in addition to improving the accuracy of wind farm power predictions. Further studies relating to the effectiveness of this model when applied to wind farm controls could be very beneficial in determining future developments to these algorithms. ~~In addition to optimizing this model's computational efficiency~~Additionally, other future work will investigate alternative interpolation methods for the ~~flow field that take into consideration~~ flow-field that consider the wind farm terrain map, capabilities for simulating more dynamic changes in wind direction, ~~and~~ implementing enforcement of momentum conservation~~for wind direction changes.~~, and optimizing the model's computational efficiency.

26
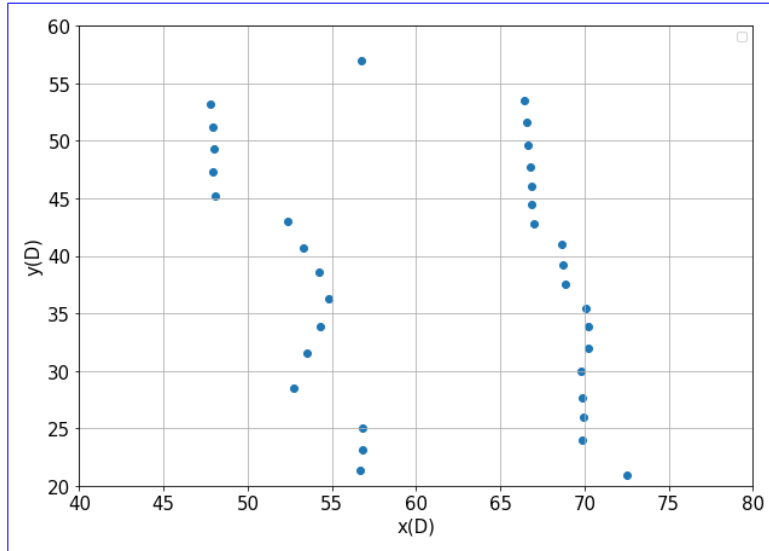
Figure A1. Map of a selected section of the wind farm, showing the inter-distance between turbine locations in the Northing (y) and Easting (x) directions. The distances shown on each axis are labeled relative to the average rotor diameter (D) of the turbines in the wind farm.

Table A1. This table lists several key attributes that characterize the nature of the terrain and turbine layout within the wind farm. Distance values are reported relative to the average turbine rotor diameter (D). Span-wise and stream-wise directions are defined to be perpendicular and parallel to the average wind direction during the wind farm, respectively.

Measured Quantity	Distance in terms of average rotor diameter (D)
Average stream-wise inter-distance	20.0 D
Average span-wise inter-distance	2.0 D
Range of elevation variation	2.2 D

27

Appendix B: Additional Results

Table B1. Analysis of wake influence. This table shows the Mean Absolute Error in total wind farm power output for three different FLORIS models, omitting FLORIS wake calculations. Total rated wind farm output was scaled to 100 MW for reference.

FLORIS Simulation Model	Mean Absolute Error for Overall Wind Farm Power Output (MW)			
	< 5 m/s	5 - 11 m/s	> 11 m/s	all
Homogeneous	4.9	26.1	38.2	22.7
Heterogeneous	4.6	28.1	13.0	18.6
Heterogeneous with Turbulence-Intensity Correction	4.0	24.9	21.9	18.5

Table B2. Analysis of wake influence. This table shows the Mean Absolute Error in individual turbine power output for three different FLORIS models, omitting FLORIS wake calculations. Total rated wind farm output was scaled to 100 MW for reference.

FLORIS Simulation Model	Mean Absolute Error in Individual Turbine Power Output (MW)			
	< 5 m/s	5 - 11 m/s	> 11 m/s	all
Homogeneous	0.045	0.244	0.198	0.152
Heterogeneous	0.0415	0.229	0.263	0.155
Heterogeneous with Turbulence-Intensity Correction	0.042	0.223	0.263	0.152

510

References

Abkar, M. and Porté-Agel, F.: Influence of atmospheric stability on wind-turbine wakes: A large-eddy simulation study, Physics of Fluids, 27, 035 104, 2015.

515 Annoni, J., Fleming, P., Scholbrock, A., Roadman, J., Dana, S., Adcock, C., Porte-Agel, F., Raach, S., Haizmann, F., and Schlipf, D.: Analysis of control-oriented wake modeling tools using lidar field results, Wind Energy Science, 3, 819–831, 2018.

Barber, C. B., Dobkin, D. P., and Huhdanpaa, H.: The Quickhull Algorithm for Convex Hulls, ACM Trans. Math. Softw., 22, 469–483, https://doi.org/10.1145/235815.235821, 1996.

Bastankhah, M. and Porté-Agel, F.: A new analytical model for wind-turbine wakes, Renewable Energy, 70, 116–123, 2014.

520 Bastankhah, M. and Porté-Agel, F.: Experimental and theoretical study of wind turbine wakes in yawed conditions, Journal of Fluid Mechanics, 806, 506–541, 2016.

Bay, C. J., Annoni, J., Martínez-Tossas, L. A., Pao, L. Y., and Johnson, K. E.: Flow Control Leveraging Downwind Rotors for Improved Wind Power Plant Operation, in: 2019 American Control Conference (ACC), pp. 2843–2848, IEEE, 2019.

Boersma, S., Doekemeijer, B. M., Gebraad, P. M. O., Fleming, P. A., Annoni, J., Scholbrock, A. K., Frederik, J. A., and van Wingerden, J.: A tutorial on control-oriented modeling and control of wind farms, in: 2017 American Control Conference (ACC), pp. 1–18, https://doi.org/10.23919/ACC.2017.7962923, 2017.

Brogna, R., Feng, J., Sørensen, J. N., Shen, W. Z., and Porté-Agel, F.: A new wake model and comparison of eight algorithms for layout optimization of wind farms in complex terrain, Applied Energy, 259, 114 189, https://doi.org/https://doi.org/10.1016/j.apenergy.2019.114189, http://www.sciencedirect.com/science/article/pii/S0306261919318768, 2020.

530 Burton, T., Sharpe, D., Jenkins, N., and Bossanyi, E. A.: Wind Energy Handbook, John Wiley and Sons, Ltd, 2002.

Chamorro, L. P. and Porté-Agel, F.: Turbulent flow inside and above a wind farm: a wind-tunnel study, Energies, 4, 1916–1936, 2011.

Clarke, A. D.: A case of shadow flicker/flashing: assessment and solution, Mechanical Engineering Publications Ltd, United Kingdom, http://inis.iaea.org/search/search.aspx?orig_q=RN:23042992, 1991.

Clifton, A. and Lundquist, J. K.: Data Clustering Reveals Climate Impacts on Local Wind Phenomena, Journal of Applied Meteorology and
535 Climatology, 51, 1547–1557, https://doi.org/10.1175/JAMC-D-11-0227.1, https://doi.org/10.1175/JAMC-D-11-0227.1, 2012.

Clifton, A. and Wagner, R.: Accounting for the effect of turbulence on wind turbine power curves, Journal of Physics: Conference Series, 524, 012 109, https://doi.org/10.1088/1742-6596/524/1/012109, 2014.

Crespo, A. and Hernández, J.: Turbulence characteristics in wind-turbine wakes, Journal of Wind Engineering and Industrial Aerodynamics, 61, 71 – 85, https://doi.org/10.1016/0167-6105(95)00033-X, 1996.

540 Dilip, D. and Porté-Agel, F.: Wind Turbine Wake Mitigation through Blade Pitch Offset, Energies, 10, 757, 2017.

Fleming, P., Annoni, J., Scholbrock, A., Quon, E., Dana, S., Schreck, S., Raach, S., Haizmann, F., and Schlipf, D.: Full-Scale Field Test of Wake Steering, in: Wake Conference, Visby, Sweden, 2017a.

Fleming, P., Annoni, J., Shah, J. J., Wang, L., Ananthan, S., Zhang, Z., Hutchings, K., Wang, P., Chen, W., and Chen, L.: Field test of wake steering at an offshore wind farm, Wind Energy Science, 2, 229–239, https://www.wind-energ-sci.net/2/229/2017/, 2017b.

545 Fleming, P., King, J., Dykes, K., Simley, E., Roadman, J., Scholbrock, A., Murphy, P., Lundquist, J. K., Moriarty, P., Fleming, K., van Dam, J., Bay, C., Mudafort, R., Lopez, H., Skopek, J., Scott, M., Ryan, B., Guernsey, C., and Brake, D.: Initial results from a field campaign of wake steering applied at a commercialwind farm – Part 1, Wind Energy Science, 4, 273–285, https://doi.org/10.5194/wes-4-273-2019, https://www.wind-energ-sci.net/4/273/2019/, 2019.

Fleming, P., King, J., Bay, C. J., Simley, E., Mudafort, R., Hamilton, N., Farrell, A., and Martinez-Tossas, L.: Overview of FLORIS updates, Journal of Physics: Conference Series, 1618, 022 028, https://doi.org/10.1088/1742-6596/1618/2/022028, https://doi.org/10.1088/1742-6596/1618/2/022028, 2020a.

Fleming, P., King, J., Simley, E., Roadman, J., Scholbrock, A., Murphy, P., Lundquist, J. K., Moriarty, P., Fleming, K., van Dam, J., Bay, C., Mudafort, R., Jager, D., Skopek, J., Scott, M., Ryan, B., Guernsey, C., and Brake, D.: Continued results from a field campaign of wake steering applied at a commercial wind farm – Part 2, Wind Energy Science, 5, 945–958, https://doi.org/10.5194/wes-5-945-2020, https://wes.copernicus.org/articles/5/945/2020/, 2020b.

Floater, M. S.: Generalized barycentric coordinates and applications, Acta Numerica, 24, 161–214, https://doi.org/10.1017/S0962492914000129, 2015.

Hamilton, N., Bay, C. J., Fleming, P., King, J., and Martínez-Tossas, L. A.: Comparison of modular analytical wake models to the Lillgrund wind plant, Journal of Renewable and Sustainable Energy, 12, 053 311, https://doi.org/10.1063/5.0018695, https://doi.org/10.1063/5.0018695, 2020.

Hedevang, E.: Wind turbine power curves incorporating turbulence intensity, Wind Energy, 17, 173–195, https://doi.org/10.1002/we.1566, 2014.

Jensen, N. O.: A note on wind generator interaction, Tech. Rep. Risø-M-2411, Risø, 1983.

Jonkman, J.: NWTC Design Codes - FAST, https://nwtc.nrel.gov/FAST, 2010.

Katic, I., Højstrup, J., and Jensen, N. O.: A simple model for cluster efficiency, in: European wind energy association conference and exhibition, pp. 407–410, 1986.

King, J., Fleming, P., King, R., Martínez-Tossas, L. A., Bay, C. J., Mudafort, R., and Simley, E.: Controls-Oriented Model for Secondary Effects of Wake Steering, Wind Energy Science Discussions, 2020, 1–22, https://doi.org/10.5194/wes-2020-3, https://wes.copernicus.org/preprints/wes-2020-3/, 2020.

Leloudas, G., Zhu, W. J., Sørensen, J. N., Shen, W. Z., and Hjort, S.: Prediction and Reduction of Noise from a 2.3 MW Wind Turbine, Journal of Physics: Conference Series, 75, 012 083, https://doi.org/10.1088/1742-6596/75/1/012083, 2007.

Martínez-Tossas, L. A., Annoni, J., Fleming, P. A., and Churchfield, M. J.: The aerodynamics of the curled wake: a simplified model in view of flow control, Wind Energy Science, 4, 127–138, https://doi.org/10.5194/wes-4-127-2019, https://www.wind-energ-sci.net/4/127/2019/, 2019.

Niayifar, A. and Porté-Agel, F.: A new analytical model for wind farm power prediction, Journal of Physics: Conference Series, 625, 012 039, https://doi.org/10.1088/1742-6596/625/1/012039, 2015.

Ning, S.: CCBlade Documentation: Release 0.1. 0, Tech. rep., National Renewable Energy Lab.(NREL), Golden, CO (United States), 2013.

NREL: FLORIS. Version 1.1.4, https://github.com/NREL/floris, 2019.

Pope, S. B.: Turbulent flows, Cambridge university press, 2000.

Schreiber, J., Bottasso, C. L., Salbert, B., and Campagnolo, F.: Improving wind farm flow models by learning from operational data, Wind Energ. Sci. Discuss., https://doi.org/10.5194/wes-2019-, in review, 2019.

Shao, Z., Wu, Y., Li, L., Han, S. J., and Liu, Y.: Multiple Wind Turbine Wakes Modeling Considering the Faster Wake Recovery in Overlapped Wakes, Energies, 12, 680, https://doi.org/10.3390/en12040680, 2019.

Sheinman, Y. and Rosen, A.: A dynamic model of the influence of turbulence on the power output of a wind turbine, Journal of Wind Engineering and Industrial Aerodynamics, 39, 329 – 341, https://doi.org/10.1016/0167-6105(92)90557-Q, 1992.

Shewchuk, J. R.: Lecture Notes on Delaunay Mesh Generation, Tech. rep., University of California at Berkeley, 1999.

Stull, R. B.: An introduction to boundary layer meteorology, vol. 13, Springer Science & Business Media, 2012.

Virtanen, P., Gommers, R., Oliphant, T. E., Haberland, M., Reddy, T., Cournapeau, D., Burovski, E., Peterson, P., Weckesser, W., Bright, J., van der Walt, S. J., Brett, M., Wilson, J., Jarrod Millman, K., Mayorov, N., Nelson, A. R. J., Jones, E., Kern, R., Larson, E., Carey, C.,

590   Polat, İ., Feng, Y., Moore, E. W., Vand erPlas, J., Laxalde, D., Perktold, J., Cimrman, R., Henriksen, I., Quintero, E. A., Harris, C. R., Archibald, A. M., Ribeiro, A. H., Pedregosa, F., van Mulbregt, P., and Contributors, S. . .: SciPy 1.0: Fundamental Algorithms for Scientific Computing in Python, Nature Methods, https://doi.org/10.1038/s41592-019-0686-2, 2020.

Yang, M., Zhang, L., Cui, Y., Yang, Q., and Huang, B.: The impact of wind field spatial heterogeneity and variability on short-term wind power forecast errors, Journal of Renewable and Sustainable Energy, 11, 033 304, https://doi.org/10.1063/1.5064438, 2019.

595   You, M., Byon, E., Jin, J. J., and Lee, G.: When wind travels through turbines: A new statistical approach for characterizing heterogeneous wake effects in multi-turbine wind farms, IISE Transactions, 49, 84–95, https://doi.org/10.1080/0740817X.2016.1204489, 2016.